CLONING, EXPRESSION, CHARACTERIZATION, AND APPLICATIONS OF ARCTIC PSEUDOMONAS PUTIDA ORIGIN (AFPA) ANTIFREEZE PROTEIN

by

ZÜLAL MUGANLI

Submitted to the Graduate School of Engineering and Natural Sciences

In partial fulfilment of

The degree requirements for degree of Master of Science

Sabancı University

December 2022

TITLE OF THE THESIS/DISSERTATION

APPROVED BY:

Asst. Prof. Dr. / Assoc. Prof. Dr. / Prof. Dr.....
(Thesis Supervisor)

Asst. Prof. Dr. / Assoc. Prof. Dr. / Prof. Dr.....

Asst. Prof. Dr. / Assoc. Prof. Dr. / Prof. Dr.....

DATE OF APPROVAL: day/month/year

ABSTRACT

CLONING, EXPRESSION, CHARACTERIZATION, AND APPLICATIONS OF ARCTIC PSEUDOMONAS PUTIDA ORIGIN (AFPA) ANTIFREEZE PROTEIN

ZÜLAL MUGANLI

Molecular, Biology, Genetics and, Bioengineering, MSc Thesis, December 2022

Thesis Supervisor: Prof. Dr. Ali Koşar

Keywords: Antifreeze Proteins, Ice Binding Proteins, Antifreeze activity, Antifreeze coating, Metallic surfaces, Aluminium surfaces, Industrial applications.

Ice formation on a solid surface is a major challenge in industrial applications, it causes higher energy consumption and performance deterioration, and might lead to catastrophic results. The preparation of anti-icing surfaces to prohibit ice accumulation on a surface is crucial to reduce operational costs and extend the surface's lifetime. The utilization of cryoprotectants to obtain anti-icing surfaces is an effective method and is applicable in multiple fields. Antifreeze proteins (AFPs) are natural cryoprotectants to obtain anti-icing surfaces having the ability to decrease the freezing point and prevent ice-crystal growth via thermal hysteresis (TH) and Ice Recrystallization Inhibition (IRI). This thesis reports the molecular cloning, expression, and production of AFP from *E. coli* via recombinant protein technology. Subsequently, produced recombinant AFPs were immobilized on aluminum surfaces by oxygen plasma to activate surface functional groups on aluminum. The anti-icing activity of the developed recombinant AFP-immobilized aluminum surfaces was evaluated. As a result, the novel coated AFP exhibited promising antifreeze activity with a high degree of anti-icing ability on aluminum surfaces. The outcome of this study provides new insight into the biotechnological application of antifreeze proteins for various industrial applications for energy-saving and higher performance.

ÖZET

PSEUDOMONAS PUTIDA KÖKENLİ (AFPA) ANTİFRİZ PROTEİNİN KLONLANMASI, EKPRESYONU, KARAKTERİZASYONU VE UYGULAMALARI

ZÜLAL MUGANLI

Moleküler Biyoloji, Genetik ve Biyomühendislik, Yüksek Lisans Tezi, Aralık 2022

Tez Danışmanı: Prof. Dr. Ali Koşar

Anahtar Kelimeler: Antifriz Protein, Antifriz etkinlik, Antifriz kaplama, metal yüzeyler, alüminyum yüzeyler, endüstriyel uygulamalar.

Endüstriyel uygulamalarda karşılaşılan, katı yüzeylerdeki buz oluşumu yüksek enerji tüketimine, cihazlarda performans düşüşüne ve felaketlere yol açabilen büyük bir sorundur. Antifriz yüzeylerin hazırlanması, yüzeylerde meydana gelen buz birikimini engelleyerek işletim maaliyetlerini azaltmada ve yüzeylerin ömrünü uzatmada kritik bir öneme sahiptir. Antifriz yüzeylerin elde edilmesi için kryoprotektan maddelerin kullanımı pek çok farklı alanda görülen etkili bir yöntemdir. Antifriz proteinler (AFP) donma noktasını düşürebilen ve buz kristalinin büyümesini termal histerezis ve rekristalizasyon inhibisyonu ile engelleyebilen doğal bir kryoprotektanlardır. Bu çalışmada, rekombinant protein teknolojisi ile AFP *E.coli* bakterisinde klonlanıp, eksprese edilmiştir. Sonrasında, üretilmiş olan AFPler, oxygen plazma ile aktifleştirilmiş olan alüminyum yüzeylere modifiye edilip ve AFP immobilize edilmiş yüzeylerin antifriz etkinliği gözlemlenmiştir. Geliştirilmiş olan AFP kaplı alüminyum yüzeyler yüksek derecede antifriz etkinliğini alüminyum yüzeylere kazandırmıştır. Bu tezin, enerji tasarrufu ve yüksek performans elde edilmesi amacıyla, AFP'lerin endüstriyel tabanlı biyoteknolojik uygulamaları için yeni bir bakış açısı kazandıracağı düşünülmektedir.

ACKNOWLEDGEMENTS

Foremost, I would like to express my sincere gratitude to my supervisor Prof. Dr. Ali Koşar for giving me this opportunity to work on my thesis, and for his able guidance and kind support throughout my master's journey.

Besides my supervisor, I would like to express my great appreciation to Dr. Ghazaleh Gharib who helped and guided me with her suggestions and precious support.

My sincere thanks go to my best friend Ayşenur Ateş, who was always with me with her brave heart and sincerity. She is always my big supporter even though she is away thousands of kilometers. I am lucky to meet with her since I found my sister.

My grateful thanks are also extended to my dearest friends; Araz Sheibani Aghdam, Atike Seyitoğlu, Eda Çapkın, Farzad Rokhsar Talabazar, Gülce Güralp, İsmail Bütün, İlayda Namlı, Jalal Karimzadeh Khoei, Mandana Mohammadilooey, Saltuk Yıldız, Serap Sakarya, Sümeyra Vural Kaymaz, Rabia Mercimek, Zeynep Eğlenen for their friendships and moral supports during my masters.

Finally, I would like to state my deepest gratitude to my meritorious family for the open-hearted support and patience they have given me throughout my education life. I am extremely lucky to have them.

Additionally, I would like to thank Scientific and Technological Research Council of Turkey (TUBITAK) since this project was supported under scope of MEraNet Project with Grant No.121N564.

December 2022 Zülal Muganlı

TABLE OF CONTENTS

LIST OF TABLES

LIST OF FIGURES

SYMBOLS

ng	Nano Gram
1X	1-fold concentrated
Kbp	Kilo Base pair
bp	Base pair
mg	Milli Gram
kDa	Kilo Dalton
mM	Milli Molar
rpm	Revolutions per Minute
µl	Micro liter
µg	Micro gram
min	Minute
abs	Absorbance
V	Volt
T	Threonine

ACRONYMS

AFPs	Antifreeze proteins
IBF	Ice binding formation
IR	Ice recrystallization
IRI	Ice-recrystallization inhibition
TH	Thermal Hysteresis
AFGP	Antifreeze Glycoproteins
3D	Three Dimensional
Pro	Proline
IBS	Ice binding site
CPA	Cryoprotective Agent
DMSO	Dimethyl Sulfoxide
P. Putida	Pseudomonas Putida
E. coli	Escherichia Coli
PDA	Polydopamine
TA	Tannic Acid
TEMED	Tetramethylethylenediamine
IPTG	Isopropyl β- d-1-thiogalactopyranoside
O.D.	Optical Density
LB	Lurian Broth
TAE	Tris-acetate EDTA
PCR	Polymerase Chain Reaction
AFP-F	Forward primer of AFP
AFP-R	Reverse primer of AFP
DNA	Deoxyribonucleic Acid
RNA	Ribonucleic Acid
SDS	Sodium Dodecyl Sulphate
SDS-PAGE	Sodium Dodecyl Sulphate Polyacrylamide Gel Electrophoresis
Tris-Cl	Trizma Chloride

CBB	Coomassie Brilliant Blue
NaCl	Sodium Chloride
CD	Circular Dichroism
Asn	Asparagine
Gly	Glycine
Cys	Cysteine
Val	Valine
Ser	Serine
Glu	Glutamic Acid
Ile	Isoleucine
Met	Methionine
Trp	Tryptophan
Thr	Threonine
Ala	Alanine
Asp	Aspartic Acid
DAQ	Data Acquisition
DSLR	Digital Single Reflex Camera
IR	Infra-Red

1. INTRODUCTION

Antifreeze proteins (AFPs) function as natural cryoprotectants and first discovered in Antarctic marine fishes in 1969 (DeVries & Wohlschlag, 1969). AFPs can be derived from several cold adaptive organisms such as, plants, bacteria, insects, algae, fungi and fishes to keep them alive under sub-zero conditions (Sutariya & Sunkesula, 2021). AFPs contains specific types of proteins, peptides and glycopeptides that have ability to bind ice while inhibiting its growth. (Baskaran et al., 2021). AFPs have six categories as, AFPs I, AFPs II, AFPs III, AFPs IV, hyperactive AFPs and anti-freezing glycoprotein AFPs according to their structural difference (John G. Duman, 2015). AFPs have ability to realize the formation of embryonic ice crystals with attaching to particular crystal planes, hence, inhibit ice growth (Olijve et al., 2016a).The action mechanism of AFPs while interacting with ice is based on depressing the water's freezing point with prevention of ice crystals' growth (Davies & Sykes, 1997; Eskandari, Leow, Rahman, & Oslan, 2020). There are plenty of antifreeze glycoproteins to inhibit ice growth, recrystallization, and nucleation. Therefore, several attempts have been done to employ AFPs as cryoprotective agents (Gharib, Saeidiharzand, Sadaghiani, & Koşar, 2022). Since, ice crystals growth is challenging for multiple fields, AFPs have been utilized in various areas such as, agriculture, anti-icing material, food industry and cryomedicine (Xiang, Yang, Ke, & Hu, 2020). However, the proteins can be easily denatured due to high temperatures, therefore it is crucial to prevent thermal denaturation to utilize them for industrial applications (Gharib et al., 2022).

1.1.Origins and Species of Antifreeze Proteins

AFPs are originated from several species such as, bacteria, fungi, plant, insects, and fishes which affects the expression and ice binding formation (IBF) of AFPs. *Moraxella* sp. of Antarctic origin was the first bacteria derived to express 52 kDa AFP which forms hexagonal ice crystals (YAMASHITA et al., 2002). *Pseudomonas fluorescens* was the first reported bacterial strain which has both antifreeze protein and ice nucleating protein activities with 80 kDa size (Kawahara et al., 2004). Arctic Plant Growth-Promoting Rhizobacterium originated *Pseudomonas putida* is another bacterial strain presenting antifreeze protein and ice nucleating protein activities with a yield of 164 kDa AFP (Naomi Muryoi et al., 2004; X. Sun, Griffith, Pasternak, & Glick, 1995b; Xu, Griffith, Patten, & Glick, 1998).

Among ciliates, *Euplotes focardii* demonstrated high ice-recrystallization inhibition (IRI) activity with efficient concentrations at nanomolar range (Mangiagalli et al., 2017). On the other hand, polar diatoms are the other species that can survive under extreme conditions, where the temperatures between -1.8 °C and -20 °C (Bayer-Giraldi, Uhlig, John, Mock, & Valentin, 2010). Gwak et al. indicated that the AFP (Cn-AFP) of *Chaetoceros neogracile*, Antarctic marine diatom, has crucial role in the low temperature adaptation and displaying antifreeze activity (I. G. Gwak, sic Jung, Kim, Kang, & Jin, 2010).

Leucosporidium sp. which is a psychrophilic yeast isolated from an Arctic pond in Norway, indicated ice-binding and IRI activities with a yield of 26 kDa (J. K. Lee et al., 2010). *Glaciozyma antarctica* PI12 is another psychrophilic yeast showed high antifreeze activity and IRI activity with having 44% α-helical secondary structure (Hashim et al., 2013). *Typhula ishikariensis* is a snow mold fungus expresses seven AFP isoforms constituting TisAFPs (Hak Jun Kim et al., 2017). Among the isoforms, the antifreeze mechanism of TisAFP6 and TisAFP8 were identified and TisAFP8 might have more effective IBF due to having higher hydrophobic structure according to TisAFP6.

Several terrestrial arthropods such as, insects, spiders, centipedes, mites express AFPs (J. G. Duman, Bennett, Sformo, Hochstrasser, & Barnes, 2004). Insect originated AFPs are represented as hyperactive AFPs since exhibiting over of 5° of Thermal hysteresis (TH) whereas polar fish are termed as moderately active due to having maximum 2° of TH activity (Meister et al., 2013a). The first identified hyperactive AFP, TmAFP, was

isolated from haemolymph of the beetle *Tenebrio molitor*, a yellow mealworm, with promising TH activity as 5°(Arai et al., 2021). *Choristoneura fumiferana*, spruce budworm, is another species that express 9kDa AFP containing β-helical structure with T-X-T motifs (Graether et al., 2000). The pale beauty moth, larvae of *Campaea perlata* expressed a hyperactive AFP since its consisting two isoforms in molecular mass of 8.3 kDa and 3.5 kDa (Lin, Davies, & Graham, 2011).

Overwintering plants express AFPs to survive in freezing conditions, besides more than 60 plants indicated antifreeze activity and 15 of them have been purified (R. Gupta & R. Deswal, 2014). A vegetable carrot, *Daucus carota*, secretes AFP consisting leucine-rich repeating units and presented IRI activity (D.-Q. Zhang, Liu, Feng, He, & Wang, 2004). From the leaf of *Secale cereale* six AFPs with different molecular masses were derived and were in homology with pathogen-related proteins (Hon, Griffith, Mlynarz, Kwok, & Yang, 1995). *Hippophae rhamnoides* (Gupta & Deswal, 2012) express AFGPs which provide the antifreeze activity in plants where their sugar group ensure IBF (Ravi Gupta & Renu Deswal, 2014).

AFPs from distinctive fish species such as teleost fish, sculpins, and winter flounder share similar structures. They generally derived from blood plasma or serum and have small molecular mass of 3-26 kDa (Tahergorabi, Hosseini, & Jaczynski, 2011). Type-I AFPs, nonglycosylated AFPs, were first discovered in *Pseudopleuronectes americanus*, winter flounder. After the discovery of several AFPs in fish, they were classified as types I, II, III, and IV. Although, the 3D structures and primary sequences are different in terms of AFP types, their ice binding activity to ice crystals are similar (H. J. Kim et al., 2017).

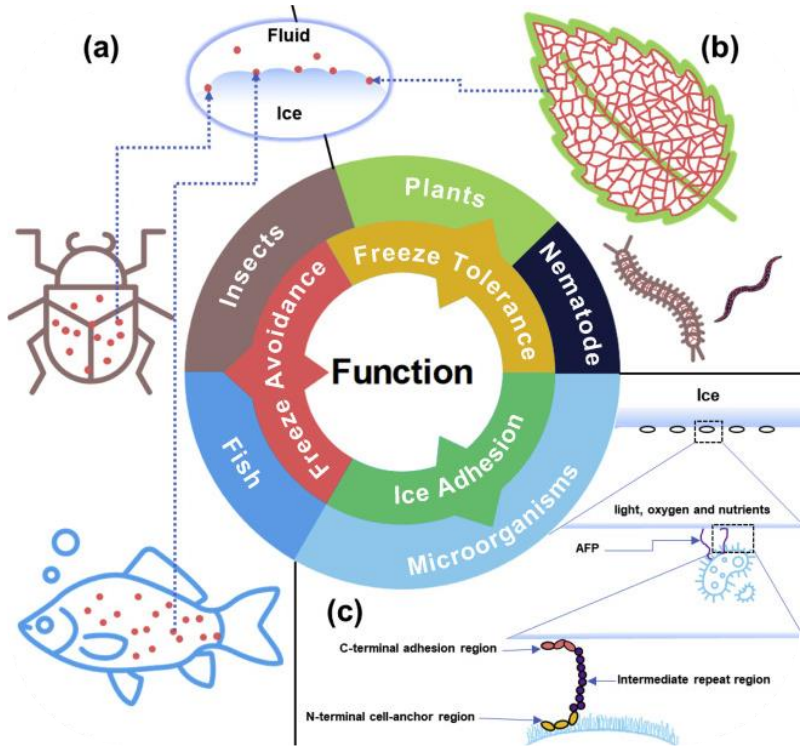

Figure 1. 1 The known biological mechanisms of AFPs from different origins. (a) Freeze avoidance, the freezing point of bodily fluids is lowered by AFPs to inhibit ice-growth, and the insects and fishes are the representative organisms. (b) In freeze tolerance, recrystallization of small ice-crystals to larger ones are inhibited by binding of AFPs to the ice crystal surfaces, like in plants, and nematode. (c) In ice adhesion, the AFPs secreted from microorganisms, work for adhesion of bacteria to ice surfaces (Xiang et al., 2020).

1.2.Classification, Structure, and Ice Plane Affinity of Antifreeze Proteins

AFPs are classified into five main classes as, AFGPs and type I, II, III, and IV according to their sources and structural differences (Eskandari et al., 2020). AFGPs are mostly expressed from some Antarctic northern cords and notothenioids and connected to the disaccharide β-d-galactosyl (1 → 3)-α-*N*-acetyl-d-galactosamine in the repetitive sequence of Ala-Ala-Thr/Arg (Mazorra-Manzano, Ramírez-Suárez, Moreno-Hernández, & Pacheco-Aguilar, 2018). Besides, AFGP isolated from some fish can have tripeptide repeats consisting proline residues (pro-thr-ala) (John G. Duman & Newton, 2020). AFGPs are classified into 8 main classes increasing size from AFGP8 (2.6 kDa) to AFGP1 (33.7 kDa). The AFGPs (1-5,7 and 8) indicated primary prisms plane binding on ice-crystals (Xiang et al., 2020). Fish AFPs are categorized into four main sections regarding to their sequences. Type I AFPs, can be expressed by plenty of fish species and contains alanine rich residues with amphipathic α-helix structure and molecular masses between 3.3 kDa and 4.5 kDa (Tejo, Asmawi, & Rahman, 2020). The type I AFPs expressed by winter flounder showed pyramidal plane binding on ice-crystals whereas

shorthorn origin Type I AFPs indicated secondary prism plane binding (Knight, Cheng, & DeVries, 1991; Wen & Laursen, 1992). Type II AFPs are cysteine-rich globular proteins having molecular masses between 11 kDa and 22 kDa and expressed by rainbow smelt, sea raven and Atlantic herring (Mazorra-Manzano et al., 2018). Modeling studies indicated that, Type II AFPs from sea ravens bind to hexagonal pyramidal plane of ice-crystals whereas type II AFPs expressed by the longsnout poacher is linked to secondary prism plane (Nishimiya et al., 2008; Wierzbicki, Madura, Salmon, & Sönnichsen, 1997). Type III AFPs are rich in β-sheet structure with 6.5 kDa size and expressed by ocean pout and wolffish. Type III AFPs have ability to dock both on the pyramidal plane and primary plane of ice-crystals (Garnham et al., 2010). Type IV AFPs are expressed by longhorn sculpin and have glutamine/glutamate rich or alanine rich residues with molecular masses of 12 kDa and 6.5 kDa, respectively. There is no data regarding to the binding of type IV AFPs to ice-crystals while having some speculations related with its essential functionality which is antifreeze activity (J. K. Lee & Kim, 2016).

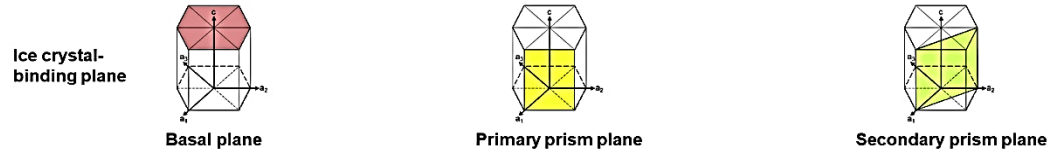

	Fish					
	Type I AFP			Type II AFP	Type III AFP	AFGP
Structure element	α-helix, Alanine rich	α-helix, Alanine rich	α-helix, Threonine-(Alanine rich)	Globular; S–S bonds	Globular; β-sandwich	AAT-repeat; Disaccharide
Representative structure				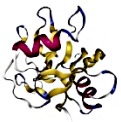	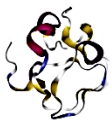	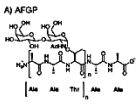
Binding plane			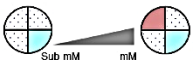	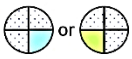		
Natural source	Winter flounder fish (wfAFP1)	Shorthorn sculpin fish (ssAFP1)	Righteye flounder, barfin plaice (bpAFP)	Longsnout Poacher sea raven, rainbow smelt, Atlantic herring	Eel pouts; ocean pout fish	Cods and Antarctic notothenii ds
Thermal hysteresis activity	Moderate	Moderate	Moderate → Hyperactive	Moderate	Moderate	Moderate
Freeze properties	Freeze avoidance					

Figure 1. 2 The figure summarizes classification, structure and ice plane affinity of AFPs (Naing & Kim, 2019).

1.3. Properties and Effects of Antifreeze Proteins

Thermal Hysteresis (TH) and Ice Recrystallization Inhibition (IRI) are the two key factors that identifies the activity of AFPs (Gharib et al., 2022). Adsorption of AFPs on to the surface of the embryonic ice crystals obstructs the enlargement of the ice crystals via decreasing the freezing point of the solution (Lopez Ortiz, Quiroga, Narambuena, Riccardo, & Ramirez-Pastor, 2021). TH can be described as the temperature gap between the melting and freezing points which indicates the activity of AFPs. TH activity has a crucial role in freeze avoidance mechanism which is vital for organisms such as plants, microalgae, bacteria and insects, to inhibit freezing of the body fluids at below 0 °C (Xiang et al., 2020). Previous studies indicated that, AFPs from insects had the highest TH values of 3-6 °C while Fish AFPs had TH values of 0.7-1.5 °C, plants and other microorganisms had TH values of 0.2-0.5 °C whereas bacteria AFPs had the lowest TH value of 0.1 °C (Baskaran et al., 2021). The TH activity of AFPs is differentiated in two classes as, hyperactive, and moderately active, and the concentration of AFP has significant impact on both TH activities. Moderately active AFPs are mostly derived from blood of polar fish with presenting maximum 2° of TH activity while hyperactive AFPs are commonly isolated from insects with presenting over 5° of TH (Meister et al., 2013b). Ice binding of hyperactive AFPs can be conducted by hydrogen binding of the hydroxyl groups of T residues. All the AFPs have comparatively hydrophobic residues in IBSs with consisting T- rich repetitive motifs while enhancing ice binding of AFPs to ice crystals consequently preventing ice growth (Vance, Bayer-Giraldi, Davies, & Mangiagalli, 2019). Hyperactive AFPs bind to prism, pyramidal and basal planes of the ice crystal and forms circular disk-like ice morphology whereas moderately active AFPs linked to prism and pyramidal planes and creates hexagonal bipyramidal ice crystal (Naing & Kim, 2019). The greater ice growth inhibition can be obtained by hyperactive AFPs since they bind to basal plane of ice and have higher TH activity according to moderately active AFPs.

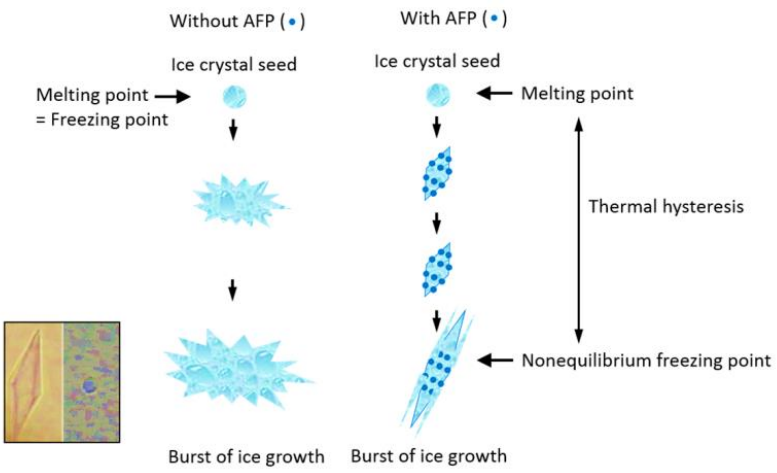

Figure 1. 3 Illustration describes the TH phenomenon of AFPs where the freezing point of water is lowered and further growth of ice crystals are inhibited until nonequilibrium freezing point (H. J. Kim et al., 2017).

Enlargement of ice crystals from the presence of the smaller ones defined as Ice Recrystallization (IR) phenomenon with Kelvin Effect (Rahman et al., 2019). IR consists of ice grain boundary migration which indicates that small ice crystals vanish whereas large ones increase in size since large ice crystals have lower free energy and thermodynamically more stable (Olijve et al., 2016b; Xiang et al., 2020). AFPs have IR inhibition (IRI) activity that prevents grain boundary migration with ceasing the growth of ice and melting it at the boundaries. AFPs can present IRI activity even at submicromolar concentrations while TH activity requires milli molar concentrations (Olijve et al., 2016b; Yu et al., 2010). Therefore, it is assumed that IRI is the primary function of AFPs secreting from the several cold-adapted organisms (Collins & Margesin, 2019). Although, both TH and IRI activity alters ice adsorption of AFPs there is no definite correlation between IRI and TH (Xiang et al., 2020). A comparative study indicated that, TH activity was not related to the activity of IRI of AFPs (Baskaran et al., 2021).

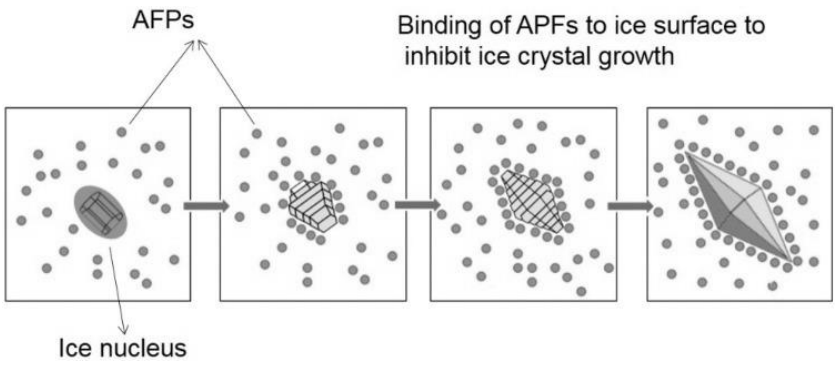

Figure 1. 4 Ice Recrystallization Inhibition effect of AFPs to the ice nucleus to prohibit ice-crystal growth(Naing & Kim, 2019).

1.4.Mechanism of Action of Antifreeze Proteins

A particular region, IBS, for protein-ice interaction is required to observe TH and IRI activities (Białkowska, Majewska, Olczak, & Twarda-Clapa, 2020). The IBSs are mostly having a flat and hydrophobic structure which is an indicator of AFPs. Although AFP might have different structures, they present common mechanism of action (Baskaran et al., 2021). Identification of ice between IBS and ice interface is vital before binding and distinguished by retarded diffusion of AFPs which is altered by their orientations specific to the surface of ice. Rigid structure of the most AFPs can be obtained by an external α-helix, internal asparagine ladders, or wide network of hydrogen bonds in the protein core (Białkowska et al., 2020). The presence of structurally similar repeating motifs in AFPs procure to form ice-binding surface with alignment of ice binding residues on one side of ice. However, to obtain adsorption between AFP and ice surface, atomic distribution of water molecules on ice crystal surface must be fulfilled by distribution of polar and apolar groups on the IBS (Smolin & Daggett, 2008). Non-binding regions of AFPs can be positioned outside and might interact with water to inhibit absorption of water by growing ice crystals. The growth rate of the ice crystal must be lower than the adsorption ratio of AFP on surface of ice to prevent enlargement of ice (Baskaran et al., 2021). Moreover, adsorption of AFP on a large area of the surface of ice crystals increases the efficiency of IRI. The affinity of AFPs to particular planes of ice crystal is related with the origin of AFPs (Białkowska et al., 2020). It is known that ice crystal growth is slower in c-axis (basal planes) than a-axis (primary prismatic plane) and AFPs with higher TH activity

bind to primary prismatic planes. This also describes the reason for growth of ice crystals in insects on the a-axis, in fish along the c-axis and in plants along the a-axis and c-axis.

1.5.Applications of Antifreeze Proteins

The advancements regarding to identification and characterization of the AFPs possessed the applications of AFPs in several fields where the growth of ice crystals induce significant challenges (Eskandari et al., 2020). The IRI and ability to decrease the freezing point of a solution makes AFPs are eligible for distinctive areas such as, cryopreservation, food industry, agriculture, and anti-icing coatings.

1.5.1. Cryopreservation

Cryopreservation is a method that ensures the storage of biologics at or below −80°C for prolonged period by use of cryo-protective agents (CPA) (Baust, Corwin, & Baust, 2011). Multiple CPAs such as, glycerol, dimethyl sulfoxide (DMSO), formamide and methanol are extensively used (Best, 2015). Since the freezing and thawing cycles are strong factors affecting the cell and organ membranes, use of high concentration of CPAs are required to minimize the intracellular ice crystal formation (Naing & Kim, 2019). However, high concentrations of CPAs might cause cellular toxicity by affecting the epigenetic regulation of cells. Therefore, alternative less or non-toxic CPAs are required to procure cryopreservation. AFPs are potential CPAs that have been demonstrated to increase cryopreservation efficacy and post thaw viability in multiple biologics (Baskaran et al., 2021). They are natural CPAs that are employed in various cryopreservation medium of oocytes (H. H. Lee et al., 2015), sperm (Beirão et al., 2012), and embryos (K. Nishijima et al., 2014). In animal models, AFPs and AFGPs prevents the cold-induced injury on cell membranes which consequently advances in vitro embryo development and survivability by altered vitrification process (Arcarons et al., 2019). Type III AFPs are extensively used AFPs for cryopreservation since its production by recombinant technology is simple (Hak Jun Kim et al., 2017). For instance, type III recombinant fish AFPs were successfully applied to enhance cryopreservation of human hepatoma cells (Hirano et al., 2008). In another study, Liang et al. (Liang et al., 2016), reported that AFGP8 had positive effects against chilling injury of bovine oocytes during vitrification procedure. Furthermore, plenty of successful applications of AFPs as CPAs were reported, AFP I and III zebrafish embryo (Martínez-Páramo, Barbosa, Pérez-Cerezales, Robles, & Herráez, 2009;

Martínez-Páramo, Pérez-Cerezales, Robles, Anel, & Herráez, 2008), AFP I in sheep embryos (Baguisi, Arav, Crosby, Roche, & Boland, 1997), LEIBP in bovine embryos (W.-S. Sun et al., 2020) and AFP III in rabbit embryos (Ekpo et al., 2022; Kazutoshi Nishijima et al., 2014).

1.5.2. Food Industry

AFPs assist in frozen food preservation by the TH and IRI activities with conserving taste and freshness of the food to prolong product shelf life (Baskaran et al., 2021). IRI activity supplies to decrease the protein oxidation, water loss and cell membrane injury whereas TH activity lowers the freezing point which obstructs denaturation of proteins. Type I AFP treatment on frozen meat procured reduction in protein loss and enhanced juiciness (Yeh, Kao, & Peng, 2009). Type III AFP treatment on actomyosin ensured protection against the freezing of gel forming functioning of muscle proteins (Boonsupthip & Lee, 2003). Besides, AFPs can be also utilized for food processing. In a comparative study, recombinant AFPs demonstrated cryoprotective activities on hydrated gluten proteins during freezing and supplied theoretical basis for dough cryopreservation (M. Liu et al., 2018). In another study, type I AFP treated frozen dough presented favourable fermentation capacity according to untreated frozen dough (Yeh et al., 2009). Kalede et al. reported that, type III AFP added ice-cream showed smoother ice cream structure and longer consumption time according to AFP concentration (Kaleda, Tsanev, Klesment, Vilu, & Laos, 2018).

1.5.3. Agriculture

Temperature is a vital factor which affects the plant growth and sub-zero temperatures induce ice-crystal formation in the apoplasts (Bredow & Walker, 2017). TH property of AFPs inhibits frost damage in the frost sensitive crops (Eskandari et al., 2020). Hence, highly active AFP expression enables to freeze at lower temperatures, nearly at 5 °C. Chilling injury in cold sensitive foods results in yield reduction and economical loss (Tian, Zhu, & Sun, 2020). To overcome with the frost damage, genetic engineering is utilized to transfer AFPs in plants. In a current study, an AFP gene from *Lolium perenne* was transferred to tomato lines (Balamurugan et al., 2018). The transformation provided, decrease in the electrolyte leakage about 2.6 times and increase in water content for 3 times. Besides, in a chilling-tolerance assay no phenotypic variation in transgenic tomato lines was observed whereas wild type lines became flattened. Moreover, AFP

transformed potato and spring wheat indicated enhanced freeze resistance with reduction of electrolyte leakage at sub-zero temperatures (Khanna & Daggard, 2006; Wallis, Wang, & Guerra*, 1997). AFPs can be employed as biofertilizer in agriculture applications. In a study, it was indicated that rhizobacterium P. Putida GR12-2 which has ability to express AFP, triggered the root growth at 5 °C (X. Sun, Griffith, Pasternak, & Glick, 1995a).

1.5.4. Industrial Applications

Formation of ice on surfaces might result in fatal accidents and serious economic loss (Baskaran et al., 2021). In this case, AFPs are favourable biomaterials to have anti- icing surfaces since they are environmentally friendly. Several coating methods such as, dip coating, spray coating, and electrodeposition can be utilized to coat AFPs on particular surfaces (Gharib et al., 2022). For instance, polymer-linked conjugation of AFPs on glass surface was employed to achieve anti-icing surface and the developed polymer coating enhanced the stability of AFPs on the glass surface (Esser-Kahn, Trang, & Francis, 2010). Gwak et al. reported that AFP coated aluminium surfaces indicated low supercooling points and addition of trehalose delayed the denaturation of AFP by formation of hydrogen bonds between hydroxyl groups of trehalose and polar residues in proteins (Y. Gwak et al., 2015; Kaushik & Bhat, 2003). In another study, an antifreeze coating was developed on glass surface by mixing antifreeze polypeptides and silane coupling agents for vehicle windshields (Koshio, Arai, Waku, Wilson, & Hagiwara, 2018). In a study conducted by Liu et al. anti-icing coating on silicon surface was developed by use of hyperactive AFP into polydopamine (PDA) and (3-glycidoxypropyl) methyldimethoxysilane (GOPTS) to understand mechanism of AFPs (K. Liu et al., 2016). Moreover, Jeonn et al. employed AFPs to create an anti-icing surfaces on PDA treated aluminum by use of Tannic acid (TA) coating (Jeong, Jeong, Nam, & Kang, 2018). Further studies are required to utilize AFPs as antifreeze coating since they can be denatured easily and lose their stability.

Research Objectives and Purpose

Ice adhesion on industrial surfaces is a major challenge that leads higher energy consumption, performance degradation and fatal incidents. Developing substrates having anti-icing properties prevent ice accumulation on a surface while extending the surface's lifetime by reducing operational costs. Cryoprotectant modified surfaces exhibits a favourable anti-icing efficiency in several fields. Among current cryoprotectants AFPs have gained a reputation due to their safety profile and innate ice-binding properties by their specific TH and IRI activities. Therefore, it is aimed to develop antifreeze metallic surfaces by use of an AFP to prohibit the ice accumulation on industrial surfaces. For this purpose, the molecular cloning, expression, and production of recombinant AFP was conducted. Subsequently, structural analysis regarding to thermal stability of the recombinant AFP and the anti-icing activity of the recombinant AFP immobilized aluminum surfaces was evaluated in this thesis. The following research plans to realize the research objectives of the design, expression, optimization and characterization of the recombinant AFP protein, immobilization of the expressed recombinant protein on aluminium surfaces and the effect of recombinant AFP immobilized aluminium surfaces on ice formation.

2. MATERIALS AND METHODS

2.1.Reagents and chemicals

Chemicals and enzymes used in this study were purchased from Sigma (USA), Merck (Germany), and Fisher Scientific (Leicestershire, UK). Restriction enzymes, DNA markers, T4 DNA ligase, DNA isolation kit and DNA extraction kits were purchased from Thermo Fisher Scientific (Massachusetts, United States), Taq DNA polymerase from Oligonucleotide primers were synthesized by Oligomer Company (Ankara, Turkey) and pUC-AFP gene was synthesized by Integrated DNA Technologies (Iowa, USA). Lurian Broth Medium, Isopropyl β- d-1-thiogalactopyranoside (IPTG), Trizma Base, Bromophenol Blue, Coomasie Blue Reagent, Sodium dodecyl sulphate, Ammonium persulfate, 30% polyacrylamide were purchased from Sigma (USA). Tetramethylethylenediamine (TEMED) was purchased from Neofroxx (Germany).

2.2.Methods

2.2.1. Cloning of the Synthetic AFP gene

2.2.1.1.Design of the synthetic AFP gene

To produce AFP, a recombinant AFP gene (1.5 kbp) was designed which has different gene sequence however encodes same amino acid sequences as original afpA, the map and open reading frame of synthetic AFP gene is shown in Fig 2.1 and Fig 2.2 (N. Muryoi et al., 2004). Therefore, it was aimed to produce large quantity of the synthesized AFP plasmid transformed in *E. coli* using recombinant technology. For this purpose, the

synthesized pUC-AFP plasmid was resuspended as it is mentioned in section 2.2.2 then transformed with *E. coli* DH5α cells as it is explained in section 2.2.3.

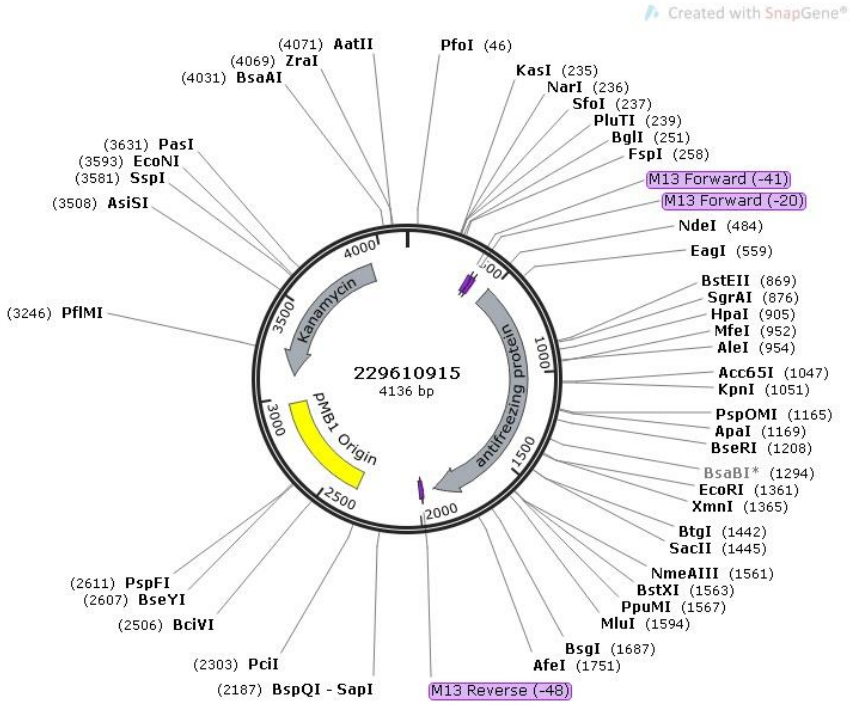

Figure 2. 1 pUC-AFP map synthesized by Integrated DNA Technology Inc.

ATGCAATACGACAGCCCAATCACTAATACCGAGTTCCAAACGTTTCTGACCACCTCCAGCATCTCCGACGACAC
CGCTGCCGCGATCAGCACTCTGCTGAACCTGGATAGCGCTGATACCATCAACCTGGCTAGCTGGGACGGCGTA
AATGCTCCGGAAATCCCAACCGGTCAGGAAGGCGCTGCTGACGTAGTAATCTAACGTTCCGGGTGCTGCTACT
GACCTGGTTCCTGTAGAAATTCCAGATTCCCTGAACTCAGCCAAAGCATTCATCTTCGATAGCAATGCAAGCCT
GGCTGTCACTTTCGATGCTCCTGTTGCCGCTGAATCGGCTTCCCTGGCTCGCGTTGCTGCTGACACGACCGCTG
GCATCGAGTTCCTGGTTACCACTGGTGCAGGCAATGACGTCATCACTGTTAATGGCGATCAGAACTCCTACATT
GACGCTGGTAACGGCAACGACACTATCGTCACTGGCAACGGCAACAACACTGTTGTGGCTGGCGCTGGTAAC
AACAACGTCACTACCGGTACCGGTAACGACACCATCATCCTGAGCGGTACTGGTCACACTGATATCGTCAACA
CTGGCGCTGGCTACGACGTGGTACAGCTGGACGGTTCGGCTGCTGACTACACCATCACCGCTGGCAACAGCAA
CAACGTCACGCTGACCGGCGCTCAAACTGCCGCGATCACTGGCGCTGAGTTCCTGACCTTCGCCGATGGCAGC
AGCGTTGCACTGGCACAAAGCGAAGCTGAAGCTTCTGCTCTGCGTCTGTACGAAGGCATCCTGGGTCGCGAC
GCTGACCAGGGCGGCGCTCAGAACTTCACGCTCAGGTTGAAGCCGGCACTGCTCTGACCGATATCGCCAATTC
GTTCCTGAACTCTGCCGAGTTCGGCGGCGCGGCAACTGAAGCTTCCATCGACAGTCTGTACACCTCCCTGTTG
GGTCGTGGTGCTGATACCGCTGGCTCGGACAGCTGGGAAGCGATCATCGCCAACGGCGGTTCGCTGGCCGATG
TAGCTGCTGGCATTGCTGGCTCTGCTGAAGCGCAAGAGCAGGATCAGTCCAACGGTACTTTCGTTGACTCCCT
GTACCTCAACGCGCTGGGCCGTCCTTCGGACGAAGCCGGTCATGACGCATGGGTAGCTCAACTGTTCAACGGC
GCAAGCCGTGCTGAAGTAGCTGCAGGCATTGTTGGTTCGGCTGAAGCTGCTGAGAAAATCAACAGCGACTTC
ATCGACGCTCTGTACCTGTCTGCTACAGGCCGTGCTTCTGACGAAGCTGGCAAAGCTGGCTGGACTGAAGTAC
TGGCTAACGGCGGCACTCAAGCTGACGTCGCTATCGGTATCGTTGGTTCGCAAGAAGCAATCGCACACAACGA
CAACGTCGTGTTCTTCACGGCGCAGTGTAA

Figure 2.2. Open Reading Frame of the recombinant AFP.

2.2.1.2. pUC-AFP Resuspension

The pUC-AFP sample preparation was performed according to the given instruction by IDT company. Therefore, first the tube containing pUC-AFP was centrifuged to ensure the plasmid is at the bottom of the tube. The plasmid was resuspended in 25 µl TE (10mM Tris, 0.1 mM EDTA) buffer (pH 8) and vortexed for 20 seconds. The suspended mixture was incubated at room temperature for 30 minutes, then centrifuged for 1 minute and stored at -20 °C for further use.

2.2.1.3. Preparation of *E. coli* competent cells and transformation

Transformation of the host plasmids (pET_{21}-MDH without tag, pET_{21}-AST without tag, pET_{28}-1699 (reference recombinant) with tag, pUC-AFP were initiated by preparing chemically competent DH5α *E. coli* strains under aseptic conditions. For this purpose, *E. coli* cells were thawed from -80 °C frozen stocks and transferred to sterile 5 ml LB medium containing tryptone, yeast extract and NaCl for overnight at 37 °C, 200 rpm then 1% of the growth was transferred to 50 ml LB medium and incubated at shaker incubator until the O.D. (600nm) reaches to 0.4 abs. The cells were harvested in a cold sterile falcon tube at 8000 rpm for 10 min at 4 °C. After centrifugation the supernatant was removed, and the cell pellet chemically induced by 50 mM cold sterile Calcium Chloride ($CaCl_2$) for 40 min on ice. The chemically induced cells were centrifuged at 8000 rpm for 10 min at 4 °C and the remaining pellet was dissolved in 50 mM ice-cold $CaCl_2$ and stored at 4 °C for transformation (Sambrook, Fritsch, & Maniatis, 1989).

An aliquot of 200 µl of DH5α competent cells were taken, and gently mixed with 5 µl of plasmids as pET_{21}-MDH, pET_{21}-AST pET_{28}-1699 and pUC-AFP and the mixture was incubated for 40 min on ice. Heat shock was applied by heat block at 42 °C for 2 min after the cells were incubated on ice for 5 min. 800 µl of LB medium was added on each plasmid group and incubated for 1 hour at 37 °C and 200 rpm. After 1 hour incubation, the 800 µl of LB medium was removed and the remaining cell suspension was mixed gently and seeded thorough LB agar plates which has proper antibiotics as,

- pET_{21}-MDH: Ampicillin (concentration:100mg/ml)
- pET_{21}-AST: Ampicillin

- pET_{28}-1699: Kanamycin (concentration: 60 mg/ml)
- pUC AFP: Kanamycin

The plates were incubated overnight at 37 °C.

2.2.1.4. Plasmid DNA isolation

The transformed plasmids were obtained by DNA isolation method and the procedure was performed with GeneJet Plasmid Miniprep kit. For this aim, one of the colonies from the transformed cell plates were selected and inoculated in LB medium with corresponding antibiotic for each group and incubated overnight at 37 °C. The prepared inoculums were harvested by centrifugation at 8000 rpm for 2 minutes. After, the supernatant was removed and 250 µl of resuspension solution was added on the cells and vortexed. Then 250 µl of lysis solution was added and the tube was inverted 4-6 times. After, 350 µl of neutralization solution was added and the tube was inverted 4-6 times. The prepared mixture was centrifugated for 5 min at 12.000 rpm at room temperature. The supernatant was transferred through flow through column and centrifugated for 1 min. The supernatant was removed and 500 µl washing solution was added and centrifugated for 1 min and repeated once more. After that empty column was centrifuged and 50 µl of elution buffer was added to columns and incubated for 4 minutes. The column was centrifugated and supernatant is collected, and concentration of collected DNA samples was measured by Nanodrop (Sambrook et al., 1989).

2.2.1.5. Quantification of DNA

Concentration of DNA constructs (pET_{21}-AFP, pET_{28}-AFP, pET_{28}-1699, pET_{21}-AST, pET_{21}-MDH, pUC-AFP) was measured spectrometrically as well as by agarose gel electrophoresis.

Spectrophotometric estimation of DNA constructs was also conducted taking the absorbance of the DNA sample at 260 nm using elution buffer as blank. Thermo Scientific NANODROP 2000c was used as spectrophotometer device to measure concentration of DNA samples. Agarose gel electrophoresis is a technique enhances to separate DNA fragments to differentiate their sizes between 100 bp to 25 kb (P. Y. Lee, Costumbrado, Hsu, & Kim, 2012). For this purpose, DNA sample was run on agarose gel along with

known amount of standard DNA of similar size. Quantification was done by comparing the intensity of DNA bands with those of standards. To prepare 0.8% agarose gel, 0.8 g of agarose was dissolved in 100 ml of 1 X TAE buffer (25 mM Tris, 5 mM sodium acetate and 1 mM EDTA pH.8) and heated in microwave until the agarose completely dissolved. After cooling to 50 ˚C of agarose solution, 2 µl GelRed nucleic acid gel stain (Biotium) was added on the dissolved agarose solution then the solution was poured into gel tray and the comb was placed to create the wells to load DNA samples. After complete solidification the gel was placed in electrophoresis tank containing 1X TAE at room temperature. 6 X DNA loading dye (Themo Scientific, #R0611) was used to mix up to 1X final concentration with DNA samples. DNA ladder, (Thermo Scientific SM1333) was used to know the size of the DNA sample. Gel electrophoresis was performed at 100 V until DNA loading dye reached one third of total gel size. BIORAD Gel Doc EZ Imager system and VILBER LOURMAT transilluminator were used to visualize and record agarose gel images.

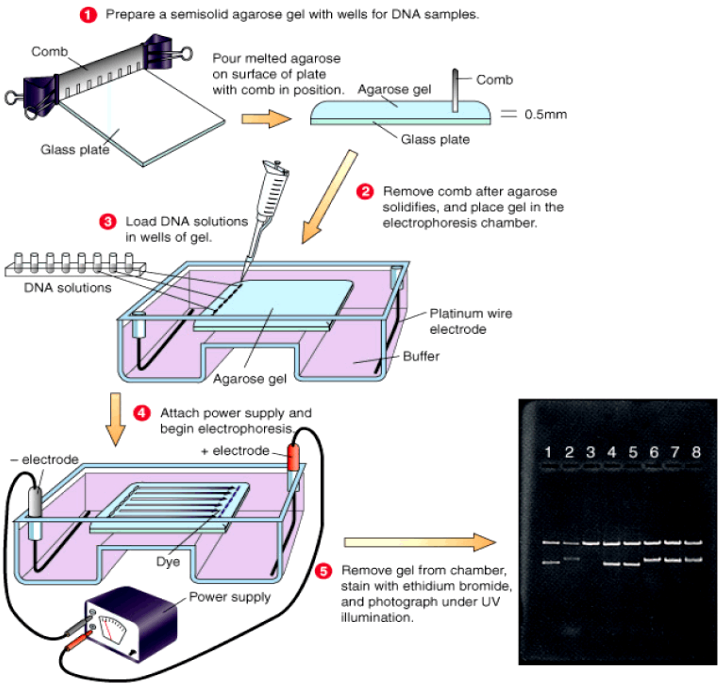

Figure 2. 1. Steps of Agarose Gel Electrophores.is to estimate size of DNA/RNA ("How to Perform DNA Electrophoresis in Agarose Gel ? ," 2022).

2.2.1.6. Polymerase chain reaction (PCR) for cloning of synthetic AFP gene

Polymerase Chain Reaction (PCR) is a method enhance to amplify specific part of the DNA template by utilizing heating and cooling cycles in presence of primers, free nucleotides, DNA template and DNA polymerase (Ghannam & Varacallo, 2018). For this purpose, PCR was performed to amplify antifreezing protein (AFP) gene by designing special RNA primers which creates Nde I (5'-CATATG-3') and Xho I (5'-CTCGAG-3') restriction sites. Herein, forward, and reverse primers (AFP-F and AFP-R) were designed according to AFP gene which is proper to create Xho I and Nde I restriction sites. The designed primers were synthesized by Oligomer Company (Ankara, Turkey). Therefore, to conduct PCR amplification, 25 µl PCR mixture was prepared which includes, 12.5 µl Taq master mixture, 1 µl forward primer (5'-ataCATATGCAGTACGATTCGCCAATTA-3'), 1 µl reverse primer (5'-ataCTCGAGTCATACCGCGCCGTGA-3'), 1.5 µl DNA template (pUC-AFP) and 9 µl nuclease free water (NF). The PCR conditions was set as in Fig 2.4.

Table 1. Designed forward primer and reverse primer of AFP. The melting Temperatures (Tm) and the Guanine-Cytosine (GC) content also is given for each primer.

Primer	Sequence (5' to 3')	Tm	GC Content
AFP-F	ataCATATGCAGTACGATTCGCCAATTA	56	36%
AFP-R	ataCTCGAGTCATACCGCGCCGTGA	61	56%

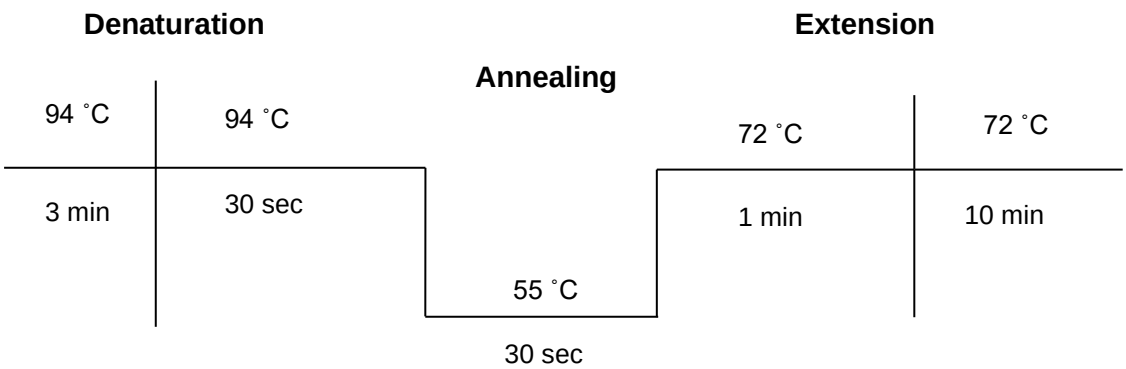

Figure 2. 2 PCR Conditions for pUC-AFP amplification.

2.2.1.7. Purification of amplified products

Amplified products were analysed by agarose gel electrophoresis and fragments of interest were excised and transferred to separate eppendorf tubes. DNA was eluted from the gel by using DNA extraction kit (Thermo Fisher Scientific). The gel slice was weighed, and one volume binding solution was added to the tube containing the gel slice. Incubation was performed at 55˚C for 10 min in a heat block device (Eppendorf, Thermo Stat plus). When the excised gel was dissolved completely, 800 µl gel solution was transferred to column and centrifuged for 1 min at room temperature. The flow though was discarded and again 100 µl of binding solution was added on the column and centrifuged. Then 700 µl of wash buffer was put on the column and centrifuged for 1 min, the flow though was discarded, and the empty column centrifuged 1 min more to remove any remaining residues. After 50 µl of elution buffer was added on the column after 5 min incubation, the column was centrifuged, the flow though was collected, and the concentrations of purified plasmids was measured by Nanodrop. Eluted DNA was then concentrated on Eppendorf concentrator 5301.DNA was quantified by taking absorbance at 260 nm using Thermo Scientific NANODROP 2000c.

2.2.1.8. Restriction analysis of recombinant plasmids

Double Digestion of pET_{21}-MDH, pET_{28}-1699 and pUC-AFP was performed by Nde I (5'-CATATG-3') and Xho I (5'-CTCGAG-3’) restriction enzymes by using Red Buffer which is the ideal buffer in case double digestion with *Nde* I and *Xho* I. For this purpose, 50 µl double digestion mixture was prepared which includes 500 ng intended plasmid, 5 µl 10x Red Buffer, 1 µl *Nde* I and *Xho* I and NF. The procedure was held in 37 °C for 1 hour.

2.2.1.9. Ligation of PCR amplified DNA in DH5α *E. coli* Cells

To create recombinant DNA plasmids (pET_{21}-AFP and pET_{28}-AFP), ligation process must be performed as two DNA fragments joins via ligase enzyme. Thus, ligation procedure was performed by using Thermo Fisher T4 ligation kit. For this purpose, 25 µl ligation mixture which consists, vector, insert, ligase, ligation buffer and NF was

prepared. The amount of vector (pET_{21} and pET_{28}) and insert (AFP gene) was evaluated according to the formula with 3:1 ratio.

$$\frac{[insert\ size(kb)]}{[vecto\ size\ (kb)]}\ x\ \frac{insert}{vector} = \frac{ng\ insert}{ng\ vector} \quad (1)$$

Table 2. Ligation reaction mixture

	Ligation Mixture Total (25 µl)	
	pET_{21}-AFP	pET_{28}-AFP
Vector	pET_{21} (1ng/µl)	pET_{28} (1.5 ng/µl)
Insert	AFP (4.5 ng/µl)	AFP (4.5 ng/µl)
Ligase	1 µl	1 µl
10x Ligation Buffer	2.5 µl	2.5 µl
Nuclease Free Water	3.93 µl	4 µl

The prepared ligation mixtures were incubated at 16 °C for overnight.

2.2.1.10. Transformation of the ligated constructs to DH5α cells

DH5α competent cell preparation and the transformation of the ligated constructs conducted as it was mentioned in section 2.2.1.3. In this experiment, there were 4 recombinant plasmid group as pET_{21}-AFP and pET_{28}-AFP which are ligated products and pET_{21}-MDH and pET_{28}-1699 as positive control groups. Each plasmid group were incubated with competent cells as it was indicated in method 2.2.1.3. After, they were spread on the agar plates which have related antibiotics, ampicillin for pET_{21}-AFP, pET_{21}-MDH and kanamycin for pET_{28}-AFP and pET_{28}-1699. Then the plates were incubated at 37 °C for overnight.

2.2.1.11. Plasmid Isolation and Confirmation by Agarose Gel Electrophoresis

To confirm the successful transformation of AFP fragment gene, the recombinant plasmid was isolated by using GeneJet plasmid isolation kit, as it was explained in section 2.2.1.4. Subsequently the resulted sample was analysed on agarose gel electrophoresis according

to 2.2.1.5. Furthermore, concentrations of isolated constructs were estimated by Nanodrop spectrophotometer.

Table 3. Concentrations of ligated recombinant products

Ligated Product	Concentration (ng/µl)
pET_{21}-AFP	138.8
pET_{28}-AFP	126.6

2.2.1.12. Restriction Digestion of Ligated Products

The ligation results of pET_{21}-AFP and pET_{28}-AFP were tested by double restriction digestion by using *Xho* I and *Nde* I restriction enzymes as it was described in section 2.2.1.8. After agarose gel electrophoresis was performed to check the presence of AFP in the ligated constructs.

2.2.1.13. Sequencing Analysis of the Cloned Genes

Sequencing analysis of recombinant DNA products were conducted by BM Labosis company. For this purpose, bidirectional sanger sequencing was utilized by using Universal T7 primers. Herein, bidirectional sequencing refers to sequencing of an initial fragment of DNA from its top and bottom strands where the top and bottom sequence reads can be matched with each other and compared (Osborne, 2015).

2.2.2. Expression of Recombinant Antifreeze Protein

2.2.2.1. Transformation of Expression Vectors to BL21 and Rosetta Cells

AFP expression was performed by transformation of pET_{21}-AFP and pET_{28}-AFP recombinant DNA constructs to *E. coli* BL21 (DE3) and *E. coli* Rosetta cells. Herein, both BL21 and Rosetta derived from *E. coli*, however due to their genetic difference

Rosetta cells have chloramphenicol resistance ability BL21 cells don't. After transformation, the formed colonies on the plates were inoculated in LB medium for overnight at 37 °C. After, the recombinant DNA constructs were isolated from the inoculation. The presence of AFP gene in recombinant constructs were indicated by double restriction digestion/ PCR amplification as described in methods 2.2.1.8. and 2.2.1.6. respectively.

2.2.2.2. Protein Production Optimization and IPTG Induction

Protein production was performed after transformation of expression vectors. For protein production, colonies were inoculated from the BL21-pET$_{21}$-AFP, BL21-pET$_{28}$-AFP and rosetta-pET$_{21}$-AFP, rosetta-pET$_{28}$-AFP containing agar plates and incubated overnight at °C, 200 rpm then 1% of the growth was transferred to 5 ml LB medium and incubated at shaker incubator until the O.D. (600nm) reaches to 0.4 abs. When O.D. was reached to 0.4, 0.5 mM IPTG induction was done on ice and the induced cell suspension was incubated at 30 C for 4 hours. At the end of the 4 hours, the cell suspension was transferred to cold falcon tubes and centrifugated at 8000 rpm, 4 °C for 10 min. The supernatant was removed, and the pellet was dissolved in Tris-Cl buffer (pH 8) to stabilize the protein content. However, to obtain a soluble protein production, the induction time by IPTG, IPTG concentration, induction temperature and the volume of the culture was optimized. IPTG induction time influences the amount of recombinant protein expression, therefore, different induction times as, 4 hours and 24 hours was applied (Hu et al., 2013). The level of the recombinant protein expression is highly affected by the IPTG concentration, different concentrations as 0.5mM, 0.8 mM and 1 mM were applied (Donovan, Robinson, & Glick, 1996). The other factor affects the protein expression, induction temperature therefore different temperatures as15 °C, 23 °C, 30 °C, 37 °C were applied on *E. coli* cells. In case of the volume optimization, AFP protein expression was first conducted from 5 ml small scale *E. coli* culture, then the volume of the culture was increased as 5 ml, 200 ml and 400 ml to increase the total protein content. The results were tested by SDS-PAGE.

2.2.2.3. Cell Lysis

Cell lysis is a method enhances to disrupt cell membrane while receiving the intercellular materials such as, protein, DNA, RNA from a cell (Shehadul Islam, Aryasomayajula, & Selvaganapathy). To reach AFP from *E. coli* cells, a probe sonicator which disrupts the cell membrane while applying ultrasonic pulses was used. For this purpose, the cell pellet which was dissolved in Tris-Cl buffer was placed in a beaker and ultrasonic pulses were applied while beaker on the ice which prevents denaturation of protein due to high temperatures. After, sonication the suspension was centrifuged the supernatant was kept in a separate falcon tube while pellet dissolved with Tris-Cl buffer in another falcon tube. After the obtained protein samples were run on SDS-PAGE to visualize the size and expression of the protein.

2.2.2.4. Analysis of AFP expression by Sodium dodecyl sulphate polyacrylamide gel electrophoresis (SDS-PAGE)

SDS-PAGE is a method procure to estimate size of proteins while denaturation of protein samples by anionic detergent sodium dodecyl sulphate (SDS) and applying electric potential to move them among polyacrylamide gel (Al-Tubuly, 2000). In this section, SDS-PAGE (12%) was prepared to analyse the size of the produced recombinant proteins produced in *E. coli*. Samples containing 1X SDS-PAGE gel loading buffer (63 mM Tris-HCl, 10% Glycerol, 2% SDS, 0.0025% Bromophenol blue, pH 6.8) were heated in boiling water for 5 min and then analysed on SDS-PAGE. Wide-mini Sub Gel GT system from BIO-RAD was used to perform sodium dodecyl sulphate polyacrylamide gel electrophoresis as described by (Laemmli, 1970). Acrylamide concentration for resolving gel was 12% and for stacking gel it was 5%. Gel was polymerized between two plates having a spacer of 1 mm. Reagents for SDS-PAGE includes:

Tris-glycine buffer (pH 8.3): Tris 3 g, glycine 18.7 g. Sodium dodecyl sulphate (SDS) 1 g, distilled water up to 1L.

Acrylamide solution (30%): Acrylamide 29 g, bis-acrylamide 1 g, distilled water up to 100 ml.

Resolving gel (12%): 2 mL of 30% acrylamide-bisacrylamide solution, 1.25 ml of 1.5 M Tris-Cl pH 8.8, distilled water 1.5 ml, 10% SDS 0.1 ml, 10% ammonium per sulphate 0.1 ml, TEMED 0.005 ml.

Stacking gel (5%): 0.5 mL of acrylamide-bisacrylamide solution, 0.38 mL of 1.5 M Tris-Cl pH 6.8, distilled water 2.1 ml, 0.03 ml of 10% SDS, 0.03 ml of 10% ammonium per sulphate and 0.003 ml of TEMED.

5X Gel loading buffer: 600ul of 1 M Tris- HCl pH 6.8, 5mL of 50% glycerol, 2ml of 10%SDS,2 mercaptoethanol 500ul,1ml of 1% Bromophenol blue distilled water up to 10 ml.

Staining solution: Coomassie brilliant blue (CBB) G250 1.25 g, glacial acetic acid 50 mL, methanol 225 ml and distilled water up to 500 ml.

Destaining solution: Glacial acetic acid 50 mL, methanol 150 mL and distilled water up to 500 ml. A comb was inserted into the stacking gel to form wells for sample loading. Electrophoresis was performed at 2 mA/cm^2 for 70-80 min until bromophenol blue dye front reached the bottom of the gel. On completion, the gel was stained with staining solution for 30 min. The gel was then destained with destaining solution to increase the visibility of protein bands.

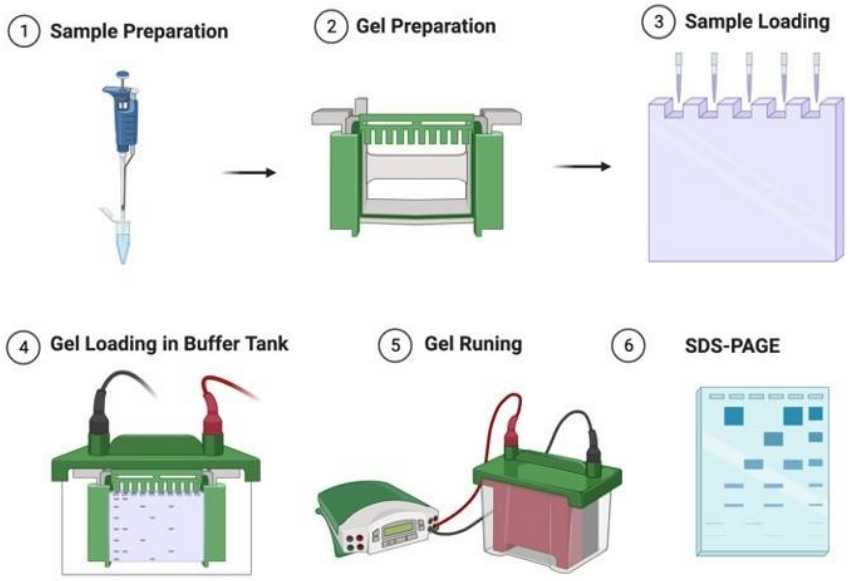

Figure 2. 3 SDS PAGE Electrophoresis Steps (Macek et al., 2019)

2.2.2.5.Estimation of protein concentration

Protein concentration of produced AFPs was estimated by using Nanodrop Bradford Assay. For this purpose, first a standard curve of the BSA was evaluated at 595 nm. Subsequently, the recombinant AFP concentration was evaluated according to the calculated equation of the standard curve.

2.2.3. Purification and Characterization

2.2.3.1. Dialysis

Dialysis is a method that works based on the diffusion of different concentrated selected solutions via non-porous membrane (E. K. Lee & Koros, 2003). Herein, dialysis was used to purify AFP while removing the salts from protein. Therefore, produced AFP samples were dialyzed against 0.5 M NaCl and 5 mM imidazole made in 20 mM Tris-HCl pH 8 buffer for overnight by using 13 kDa dialysis tubing. The process was performed at 4 C to prevent protein denaturation.

2.2.3.2.Nickel affinity chromatography only for tagged AFP

The supernatant after heat treatment containing recombinant pET_{28}-AFP was dialyzed against 0.5 M NaCl and 5 mM imidazole made in 20 mM Tris-HCl pH 8 buffer for overnight and then applied to high-capacity nickel chelate affinity matrix Ni-CAM HC Resin (Sigma) column which was equilibrated with the same buffer. The bound proteins were gradually eluted with 5 mM, 10 mM, 50 mM, 100 mM, 150 mM, 200 mM, 250 mM, and 300 mM imidazole. The eluted protein samples were analysed by SDS-PAGE as described above in section 2.2.

2.2.3.3.Gel filtration chromatography

Gel filtration chromatography also known as size exclusion chromatography enhance to separate molecules in a sample according to their molecular size with the help of the pores of the gel filtration medium (Prapulla & Karanth, 2014). Gel filtration

chromatography was utilized to purify AFP according to the size of the molecules. For this purpose, size exclusion chromatography columns which include gel filtration medium was used. The column first washed by Tris-Cl buffer. After the protein sample was loaded on the column and the drop were collected and analysed by SDS-PAGE.

2.2.3.4.Circular Dichroism (CD) Spectroscopy and Thermal Stability Analysis

Secondary structure analysis of AFP was evaluated by CD spectroscopy measurements by Jasco J-810 CD Spectrophotometer. The process was conducted according to Marshall et al. (Marshall, Chakrabartty, & Davies, 2005). Briefly, the AFP sample was dialyzed against 10 mM Tris-chloride buffer (pH 8.0) at 4 °C. The dialysis buffer was scanned to establish the baseline CD. Wave scans were obtained between 180 nm and 260 nm by sampling the data at 1.0-nm and 50nm/min scanning rate. The results were defined as mean residue molar ellipticity (deg·cm^2/dmol). The thermal stability analysis was carried out by CD spectroscopy to determine the effect of temperature fluctuations on secondary structure of AFP. For this aim, several scans were obtained at multiple temperatures (-8, -4,0,4,8, 10, 20, ,30, ,40, 50, and 60).

2.2.3.5. Structure Prediction and Homology Modeling

The amino acid sequence of *Pseudomonas putida* afpA gene for antifreeze protein was retrieved from the website of the National Centre for Biotechnology Information (http://www.ncbi.nlm.nih.gov/) https://www.ncbi.nlm.nih.gov/nuccore/AJ784158 and was used as a query sequence for the structure prediction and homology modeling. The sequence was submitted to NCBI Blast (http://blast.ncbi.nlm.nih.gov/Blast.cgi) to get the most similar protein whose structure had been determined. Among the proteins whose structure has been determined AFP from cyanobacterial phycobilisome from Anabaena sp. PCC 7120 was found most similar with a homology of 20 percent therefore it was used as a template for structure prediction and homology modeling studies.

2.2.4. The Recombinant AFP immobilization on Aluminium Surfaces

The expressed AFP was coated on metallic surfaces by oxygen plasma. For this aim, the metallic surfaces treated by oxygen plasma for 1 min to activate functional groups on the surfaces and enhance cross-linking, as shown in Fig 1 (De Geyter & Morent, 2014). After AFP containing tris-chloride solution was coated on the treated metallic surfaces and all the procedure while coating was conducted on ice.

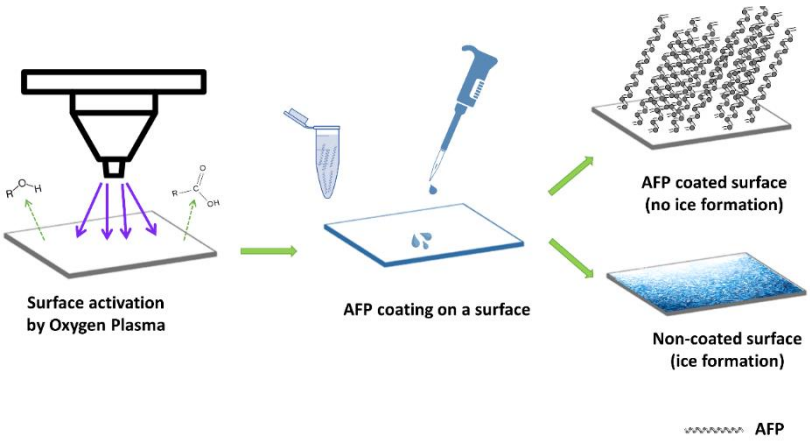

Figure 2. 4. Recombinant AFP coating on metallic surfaces enhanced by oxygen plasma.

2.2.5. Antifreeze Activity Tests of AFP coated Aluminium Surfaces

The activity of produced recombinant AFP and the anti-icing activity of the immobilized recombinant AFP were characterized using a lab-made test section. The setup composed of a closed chamber with relative humidity and temperature regulator, a power supply to regulate the temperature (supercooling temperature) of the tested specimen, temperature and humidity sensors, a data acquisition system (DAQ), a light source, a high-speed, a DSLR, and an IR thermal camera. The schematic of the experimental setup is given in the appendix 5.

3. RESULTS

3.1. Transformation of recombinant plasmid pUC-AFP with Escherichia coli (E. coli) DH5α Cells

Competent cell preparation and transformation was conducted as it mentioned in method 2.2.1.3. Therefore, first DH5α cells were inoculated from -80 °C frozen stocks to sterile 5 ml LB medium for overnight then 1% of the growth was transferred to 50 ml LB medium and incubated at shaker incubator until the O.D. (600nm) reaches to 0.4 abs. The cells were chemically induced by $CaCl_2$ and 200 µl of competent cells were transferred to eppendorf tubes for each plasmid group as; pET_{21}-MDH, pET_{21}-AST pET_{28}-1699 and pUC-AFP. Based on our results, the pET_{21}-MDH and pET_{21}-AST colonies indicating host ampicillin resistance were observed on plates indicating the expression of cloning vector relevant proteins which are shown in Fig 4 and Fig 5, respectively. Furthermore, pET_{28}-1699 and pUC-AFP colonies which demonstrates kanamycin resistance were observed on plates and can be seen in Fig and Fig respectively. The difference of number of colonies between the groups are due to the concentration difference of the plasmids, since high concentration of plasmid forms higher number of colonies. However, the results were indicated that the transformation of plasmids pET_{21}-MDH, pET_{21}-AST pET_{28}-1699 and pUC-AFP to DH5α cells was successful since each plasmid group grow on related antibiotic plates as positive control groups whereas bare competent cells did not grow on antibiotic plates as negative control groups.

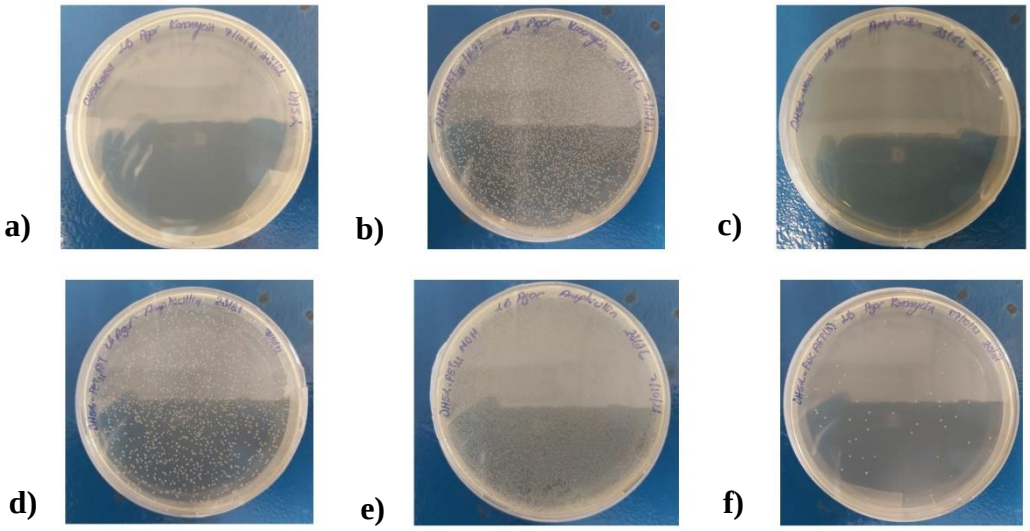

Figure 3. 1. Transformation results of recombinant plasmid pUC-AFP with E. coli DH5α Cells a) DH5α competent cells on Kanamycin Plate (Negative Control). b) DH5α competent cells transformed withpET$_{28}$-1699 on Kanamycin Plate (Positive Control). c) DH5α competent cells on Ampicillin Plate (Negative Control). d) DH5α competent cells transformed with pET$_{21}$-AST on Ampicillin Plate (Positive Control). e) DH5α competent cells transformed with pET$_{21}$-MDH on Ampicillin Plate (Positive Control). f) DH5α competent cells transformed with pUC-AFP on Kanamycin Plate (Positive Control).

3.1.1. Plasmid DNA Isolation

The plasmid isolation was performed according to the section 2.2.1.4. The size of isolated plasmids was evaluated by agarose gel electrophoresis and Nanodrop device as it was mentioned in 2.2.1.5. The results were indicated that the isolated plasmids were in expected size as, pET$_{21}$-MDH was in 5.4 kb, pET$_{21}$-AST in 5.443 kb, pET$_{28}$-1699 in 5.369 kb and pUC-AFP is around 4.1 kb.

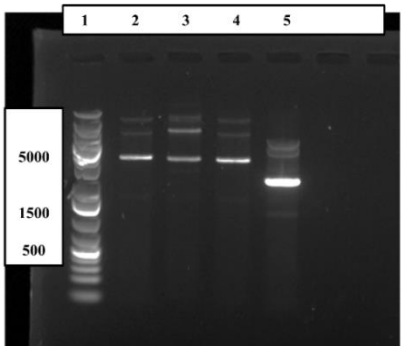

Figure 3. 2 Gel red stained 0.8% agarose gel showing plasmid DNA isolated from four different colonies. Lane 1, molecular marker (SM01333); lane 2, pET$_{21}$-AST; lane 3, pET$_{21}$-MDH; lane 4, pET$_{28}$-1699 and lane 5, pUC-AFP.

3.1.2. Polymerase Chain Reaction (PCR) Amplification of pUC-AFP

PCR amplification of pUC-AFP was performed as mentioned in method 2.2.1.6. The PCR amplification was confirmed by agarose gel electrophoresis. The results were demonstrated that, AFP gene was successfully amplified by PCR amplification which can be shown in Fig 3.3 since the size of AFP is 1.5 kb.

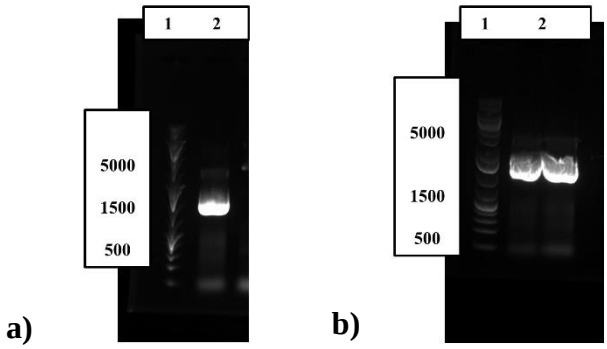

Figure 3. 3. Gel red stained 0.8% agarose gel showing, a) Lane 1, molecular marker (SM1333 Lane 2, PCR Product of pUC-AFP (1.5 kbp) b) Lane 1, molecular marker (SM1333) Lane 2, PCR Product of pUC-AFP (1.5 kbp)

3.1.3. Restriction analysis of recombinant plasmids

Double restriction digestion of pET_{21}-MDH, pET_{28}-1699 and pUC-AFP was performed as it described in section 2.2.1.8. The restriction digestion was analysed by agarose gel electrophoresis and the results were confirmed that double restriction of pET_{21}-MDH, pET_{28}-1699 and pUC-AFP was successful since, pET_{21} in 5.4 kb, pET_{28} in 5.4 kb and AFP in 1.5 kb.

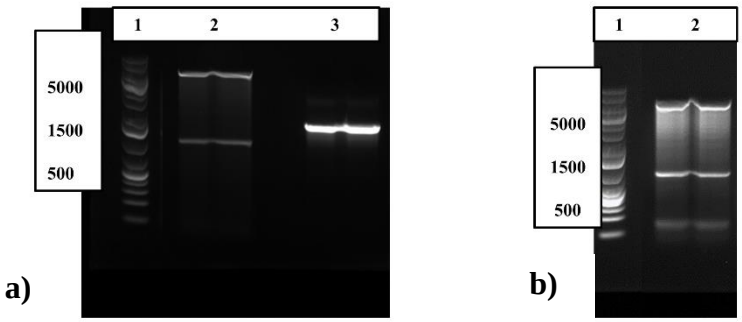

Figure 3. 4 a) Gel red stained 0.8% agarose gel showing: Lane 1, molecular marker (SM1333), Lane 2, pET 28-1699 Double Restricteed, Lane 3, pUC-AFP Double Restricted. b) Gel red stained 0.8% agarose gel: Lane 1, molecular marker (SM1333), Lane 2, pET_{21}-MDH Double Restricted.

3.1.4. Ligation of PCR amplified AFP to DH5α Cells

Ligation procedure of pET_{21}-AFP and pET_{28}-AFP was conducted as it was explained in part 2.2.1.9. Based on our results, the pET_{21}-AFP and pET_{21}-MDH colonies indicating host ampicillin resistance were observed on plates indicating the expression of cloning vector relevant proteins which are shown in Fig 17 and Fig 18, respectively. Furthermore, pET_{28}-AFP and pET_{28}-1699 colonies which demonstrates kanamycin resistance were observed on plates and can be seen in Fig 16 and Fig 19 respectively. As a result, transformation of pET_{21}-AFP and pET_{28}-AFP was successful since colonies were observed on plates while there was no colony in negative controls which includes only competent cell on ampicillin plate as it is shown in Fig 3.5.

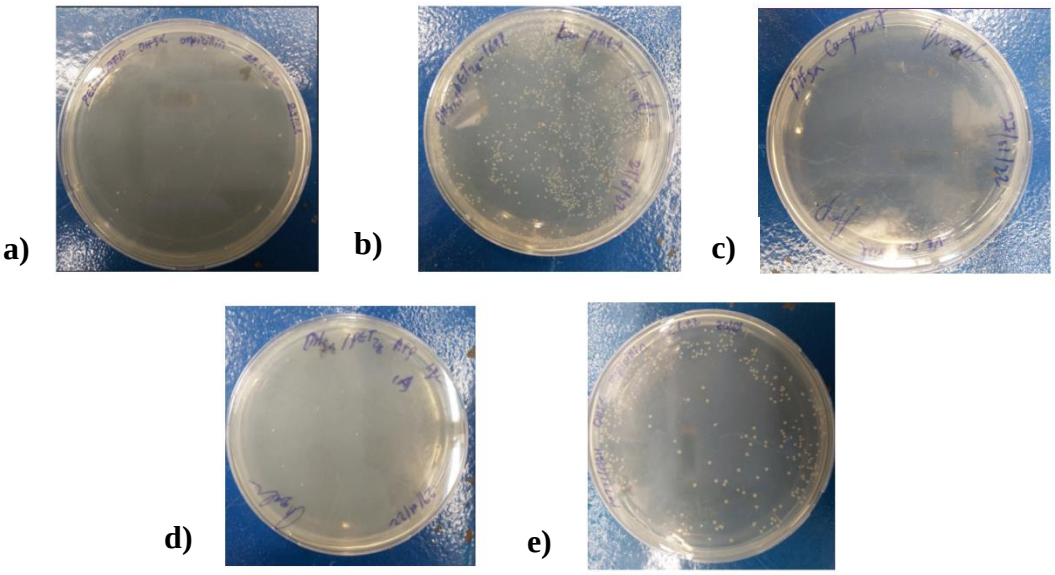

Figure 3. 5 a) DH5α-pet21-afp on ampicillin plate b) DH5α-pet28-1699 on kanamycin plate c) DH5α competent cells on ampicillin plate. d) DH5α-pet28-afp on kanamycin plate e) DH5α-pet21-mdh on ampicillin plate.

3.1.5. Plasmid Isolation of Ligated AFP products

The agarose gel results were indicated that both ligated plasmids, pET_{21}-AFP and pET_{28}-AFP were in expected size which is around 7 kb as it is demonstrated in Fig 3.6. This result indicated the presence of AFP in both constructs since AFP in 1.5 kb size, pET_{21} and pET_{28} are around 5.4 kb size.

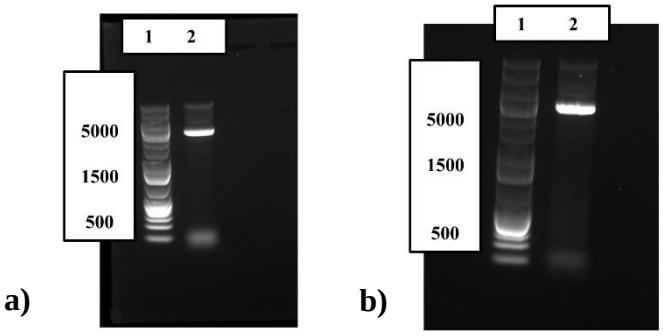

Figure 3. 6 a) Gel red stained 0.8% agarose gel showing; Lane 1, molecular marker (SM1333); Lane 2, pET_{28}-AFP b) Gel red stained 0.8% agarose gel showing; Lane 1, molecular marker (SM1333); Lane 2, pET_{21}-AFP.

3.1.6. Restriction Digestion of Ligated Products

The agarose gel results were confirmed that the ligation of pET_{21}-AFP and pET_{28}-AFP was successful since AFP gene can be barely seen in the 1.5 kb band for both constructs. Besides, the vectors pET_{21} and pET_{28} were in the expected size which is around 5.4 kb as it is shown in Fig 3.7.

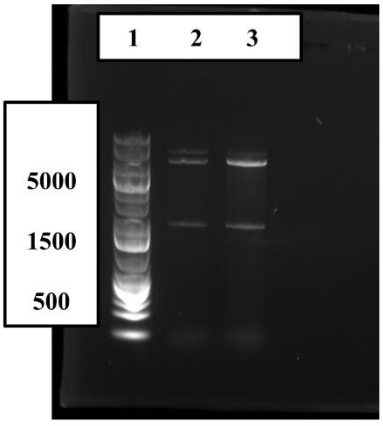

Figure 3. 7 Gel red stained 0.8% agarose gel showing; Lane 1, molecular marker (SM1333); Lane 2, pET 28-AFP Double Restricte, Lane 3, pET21-AFP Double Restricted.

3.1.7. Sequencing Analysis of the Cloned Genes

Sequencing analysis was performed as it was mentioned in method of 2.2.1.1.3. The analysis results were demonstrated that, for both plasmid constructs the ligated parts as pET_{21} and AFP, and pET_{28} and AFP were in correct order. The data is shown for pET_{28}-

AFP and pET_{21}- AFP in Fig 3.8. and Fig 3.9. respectively. The sequencing analysis results were given in the appendix 1,2,3,4.

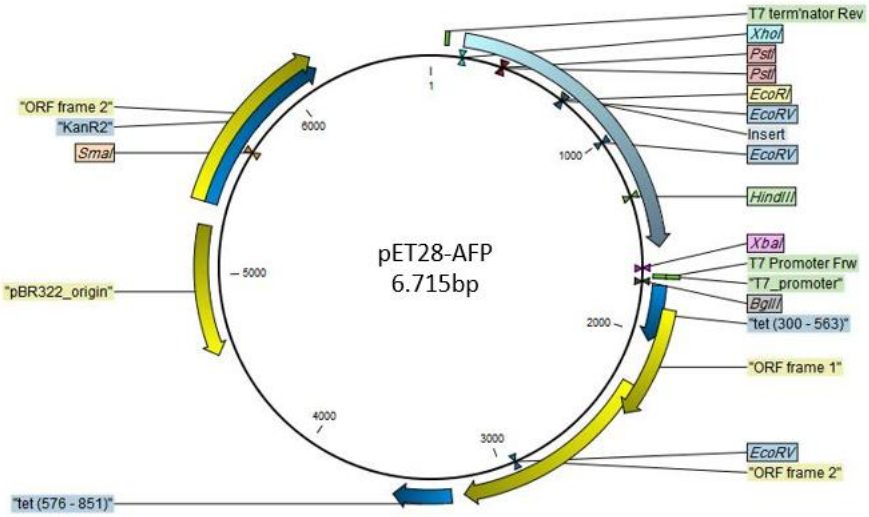

Figure 3. 8 Sequencing analysis results of pET_{28}-AFP construct.

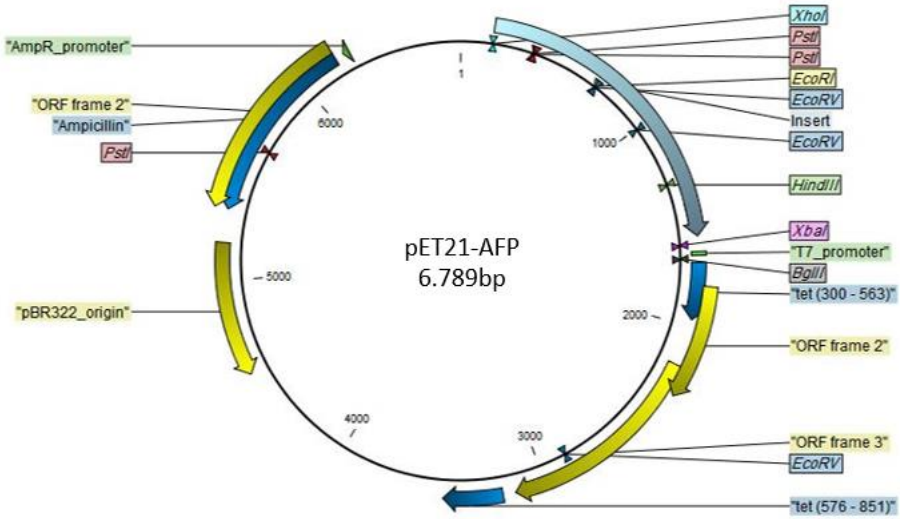

Figure 3. 9 Sequencing analysis results of pET_{21}-AFP construct**.**

3.1.8. Transformation of pET_{21}-AFP and pET_{28}-AFP Products with BL21 *E. coli* Cells for Protein Expression

The isolated recombinant pET_{21}-AFP and pET_{28}-AFP were transformed to BL21 cells to express AFP. The results were indicated that transformation to BL21 cells was successful. Since there was colony formation in ampicillin plates and kanamycin plates while pET_{21}-

AFP is having ampicillin resistance and pET_{28}-AFP is having kanamycin resistance, respectively.

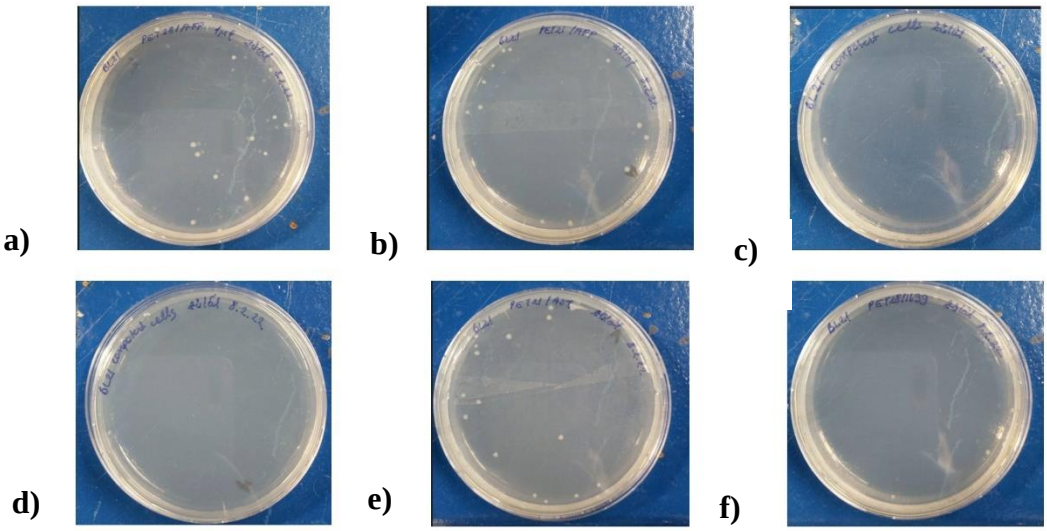

Figure 3. 10 a) BL21-pET_{28}-AFP competent cells on Kanamycin Plate (Positive Control), b) BL21-pET_{21}-AFP competent cells on Ampicillin Plate (Positive Control) c) BL21 competent cells on Kanamycin Plate (Negative Control) d) BL21 competent cells on Ampicillin Plate (Negative Control) e) BL21-pET_{21}-AST competent cells on Ampicillin Plate (Positive Control) f) BL21-pET_{28}-1699 competent cells on Kanamycin Plate (Positive Control)

3.1.9. Plasmid isolation of transformed Constructs

Agarose gel electrophoresis was performed to evaluate size of isolated pET_{21}-AFP and pET_{28}-AFP constructs. The results were demonstrated that, the size of isolated recombinant plasmids was in correct size since pET_{21}-AFP and pET_{28}-AFP in around 7kb size as it was shown in fig 3.11.

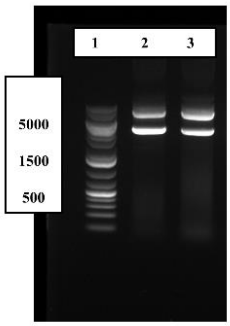

Figure 3. 11 Gel red stained 0.8% agarose gel showing; Lane 1, molecular marker (SM1333), Lane 2, pET_{21}-AFP; Lane 3, pET_{28}-AFP.

3.1.10. Rosetta Transformation Results of Ligated pET_{21}-AFP and pET_{28}-AFP Products for Protein Expression

The isolated recombinant pET_{21}-AFP and pET_{28}-AFP were cloned to *E. coli* Rosetta cells to express AFP. The results were indicated that transformation to Rosetta cells was successful. Since there was colony formation in ampicillin plates and kanamycin plates while pET_{21}-AFP is having ampicillin resistance and pET_{28}-AFP is having kanamycin resistance, respectively.

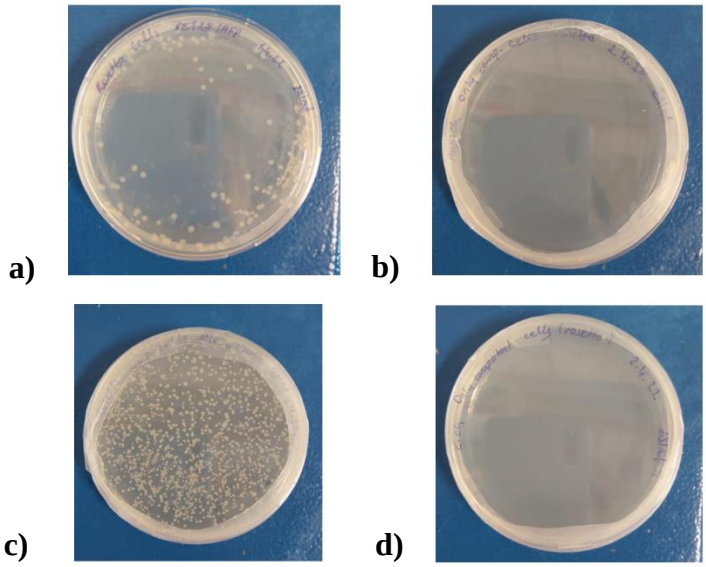

Figure 3. 12 a) Rosetta-pET28-AFP competent cells on Kanamycin/chloramphenicol Plate (Positive Control) b) Rosetta competent cells on ampicillin/chloramphenicol Plate (Negative Control) c) Rosetta-pET21-AFP competent cells on Chloramphenicol/Ampicillin Plate (Positive Control) d) Rosetta competent cells on kanamycin/chloramphenicol Plate (Negative Control).

3.1.11. Plasmid Isolation of Transformed Constructs

PCR amplification was performed to check the presence of AFP gene in pET_{21}-AFP and pET_{28}-AFP constructs. After, agarose gel electrophoresis was performed to evaluate size of amplified AFP in pET_{21}-AFP and pET28-AFP constructs. The agarose gel electrophoresis results were confirmed that AFP gene is present in pET_{21}-AFP and pET_{28}-AFP constructs which are shown in 5th and 7th lanes in corresponding size of 1.5kbp in the fig 3.13.

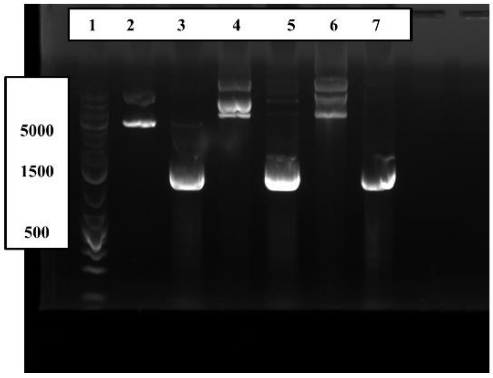

Figure 3. 13 Gel red stained 0.8% agarose gel showing; Lane 1, molecular marker (SM1333), Lane 2, pUC-AFP; Lane 3, pUC-AFP PCR, Lane 4, pET_{21}-AFP, Lane 5, pET_{21}-AFP PCR, Lane 6, pET_{28}-AFP, Lane 7, pET_{28}-AFP PCR.

3.2. Analysis of AFP expression by Sodium dodecyl sulphate polyacrylamide gel electrophoresis (SDS-PAGE)

3.2.1. Induction Time

Two different induction time as 4 hours and 24 hours was applied for induction of AFP protein. The SDS PAGE results were indicated that 4 hours induction time is favourable to express AFP since 24 hours induction time caused degradation of AFP protein.

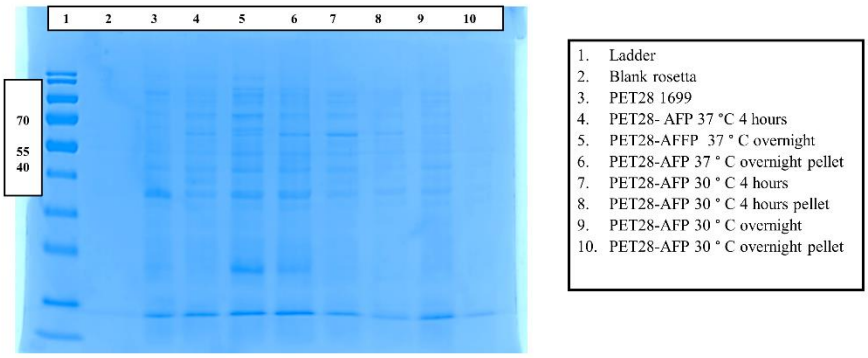

Figure 3. 14 SDS PAGE (12%), stained with Coomassie blue, SDS gel shows AFP expression of pET_{21}-AFP and pET_{28}-AFP by inducing them at 37 °C and 30 °C for 4 hours and overnight. The size of the AFP protein is between 55-70kDa

3.2.2. Temperature

Different induction temperatures as, 15 °C, 23 °C, 30 °C, 37 °C were applied on *E. coli* cells. The SDS PAGE results were indicated that 30 °C IPTG induction temperature is ideal to express AFP from pET_{21}-AFP and pET_{28}-AFP since the protein expression can be seen clearly in 30 °C samples.

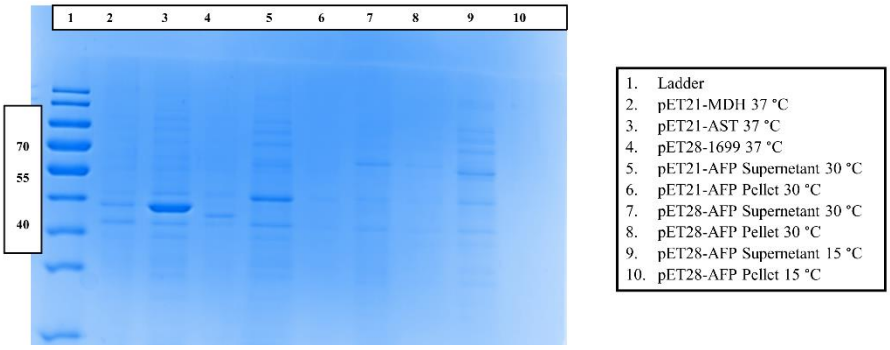

Figure 3. 15 SDS PAGE (12%), stained with Coomassie blue, all the samples were induced by 0.5mM IPTG. SDS gel shows AFP expression of pET_{21}-AFP and pET_{28}-AFP with induction at 30 °C and 15 °C. The size of the AFP protein is between 55-70kDa.

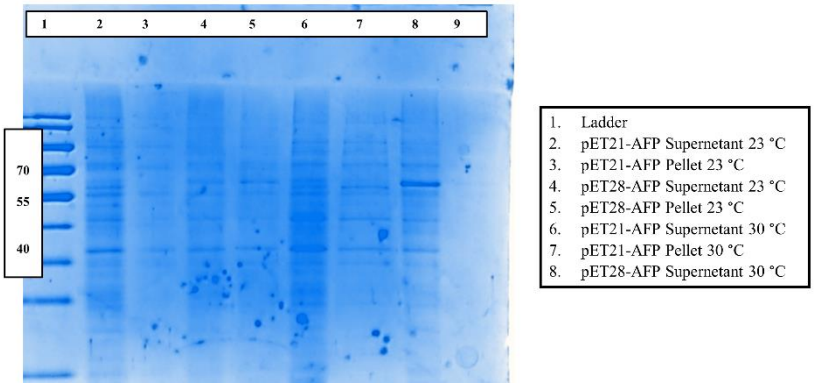

Figure 3. 16 SDS PAGE (12%), stained with Coomassie blue, all the samples were induced by 0.5mM IPTG. SDS gel shows AFP expression of pET_{21}-AFP and pET_{28}-AFP by inducing them at 23 °C and 30 °C. The size of the AFP protein is between 55-70kDa

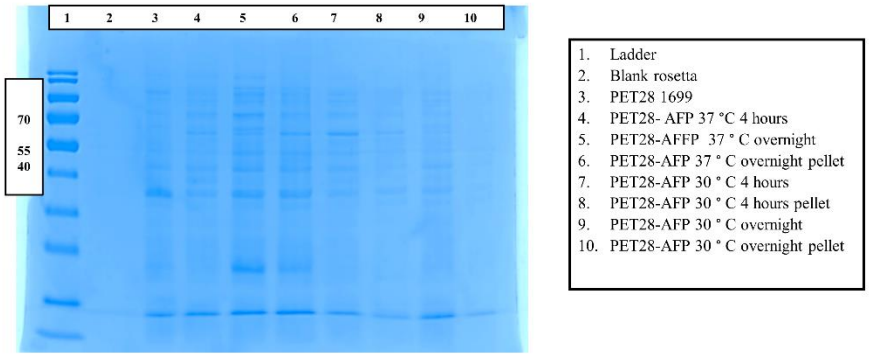

Figure 3. 17 SDS PAGE (12%), stained with Coomassie blue, all the samples were induced by 0.5mM IPTG. SDS gel shows AFP expression of pET_{21}-AFP and pET_{28}-AFP with induction at 37 °C and 30 °C. The size of the AFP protein is between 55-70kDa.

3.2.3. IPTG Concentration

Different IPTG concentrations as 0.5 mM, 0.8 mM and 1mM were applied for induction of AFP protein. The results were demonstrated the 0.5 mM IPTG induction is ideal to initiate induction of pET_{21}-AFP and pET_{28}-AFP according to SDS PAGE results.

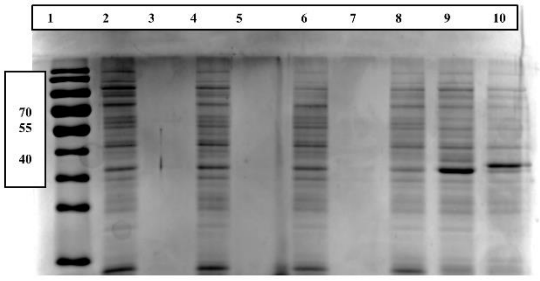

1. Ladder
2. pET21- AFP Supernetant, 0.5 mM IPTG, 37 °C
3. pET21-AFP Pellet, 0.5 mM IPTG, 37 °C
4. pET21-AFP Supernetant, 0.5 mM IPTG, 18 °C
5. pET21-AFP Pellet, 0.5 mM IPTG 18 °C
6. pET21-AFP Supernetant,0.8 mM, 18 °C
7. pET21-AFP Pellet, 0.8 mM, 18 °C
8. pET21-AFP Supernetant 1 mM, 18 °C
9. pET21-MDH, 0.5 mM, 37 °C
10. pET28-1699, 0.5 mM, 37 °C

Figure 3. 18 SDS PAGE (12%), stained with Coomassie blue, SDS gel shows AFP expression of pET_{21}-AFP and pET_{28}-AFP by inducing them at 37 °C and 18 °C by inducing them 0.5mM, 0.8 mM and 1mM IPTG. The size of the AFP protein is between 55-70kDa.

3.2.4. Volume of culture

Different culture volumes as 5ml, 200 ml and 400 ml was used to express AFP. The SDS PAGE results were demonstrated the there was a small amount of AFP production in 5ml culture, while large cultures as 200 ml and 400 ml had large amount of AFP expression.

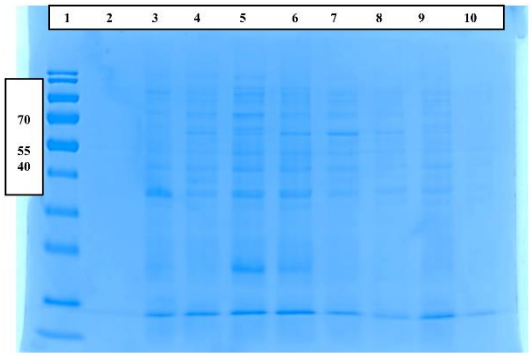

1. Ladder
2. Blank rosetta
3. PET28 1699
4. PET28- AFP 37 °C 4 hours
5. PET28-AFFP 37 ° C overnight
6. PET28-AFP 37 ° C overnight pellet
7. PET28-AFP 30 ° C 4 hours
8. PET28-AFP 30 ° C 4 hours pellet
9. PET28-AFP 30 ° C overnight
10. PET28-AFP 30 ° C overnight pellet

Figure 3. 19 SDS PAGE (12%), stained with Coomassie blue, SDS gel shows AFP expression of pET_{28}-AFP from 5ml culture.

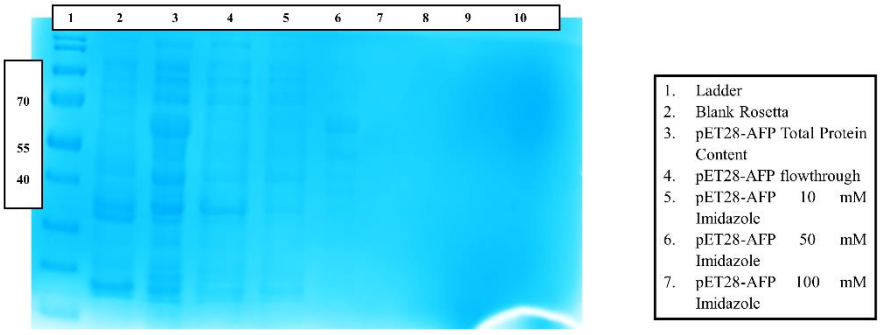

Figure 3. 20 SDS PAGE (12%), stained with Coomassie blue, SDS gel shows AFP expression of pET_{28}-AFP from 200ml culture. The size of the AFP protein is between 55-70kDa

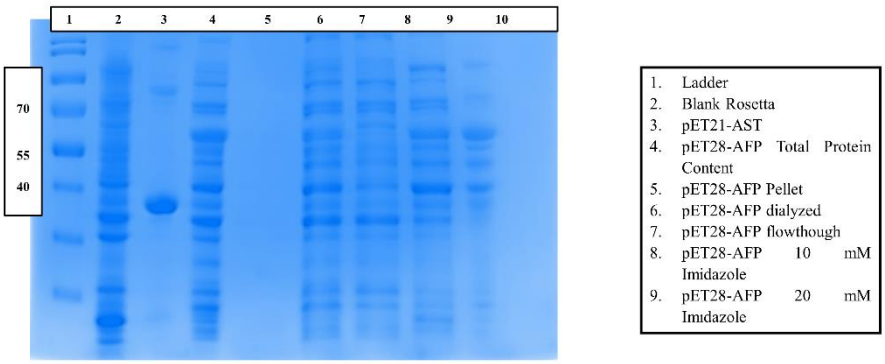

Figure 3. 21 SDS PAGE (12%), stained with Coomassie blue, SDS gel shows AFP expression of pET_{21}-AFP from 400ml culture which was induced by 0.5 mM IPTG at 30 °C for 4 hours. The size of the AFP protein is between 55-70kDa

3.3. Results of Purification and Characterization

3.3.1. Dialysis

Dialysis applied to remove excessive amount of salt from the AFP construct. Figure 3.22 shows the dialyzed sample of pET_{28}-AFP with expected lower concentration according to the total protein content.

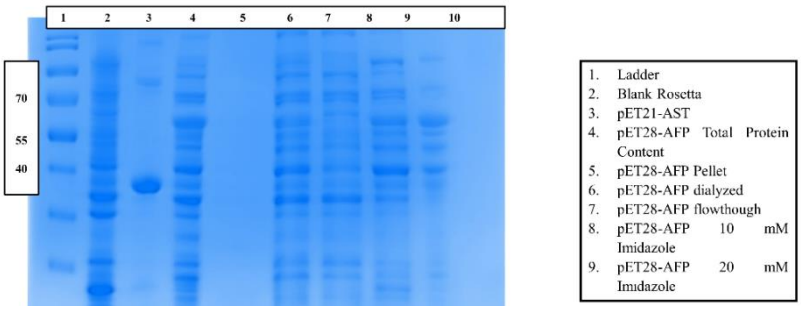

Figure 3. 22 SDS PAGE (12%), stained with Coomassie blue, SDS gel shows AFP expression of pET_{21}-AFP from 400ml culture which was induced by 0.5 mM IPTG at 30 °C for 4 hours. The size of the AFP protein is between 55-70kDa. The Lane 6 indicates dialyzed sample.

3.3.2. Nickel Affinity Chromatography

Nickel affinity chromatography was applied for tagged AFP expression which is pET_{28}-AFP. According to results of SDS PAGE, partially purified pET_{28}-AFP was obtained after 50mM imidazole treatment.

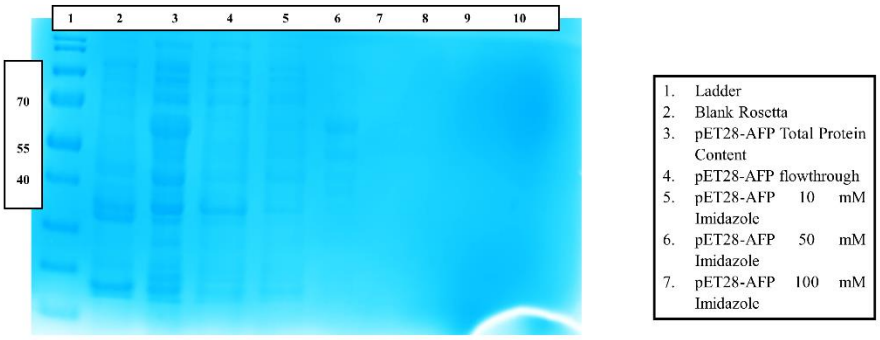

Figure 3. 23 SDS PAGE (12%), stained with Coomassie blue, SDS gel shows AFP expression of partially purified pET28-AFP from 200ml culture which was induced by 0.5 mM IPTG at 30 °C for 4 hours. The size of the AFP protein is between 55-70kDa

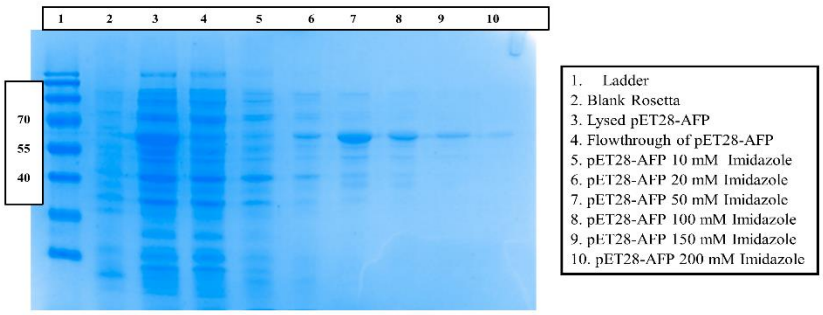

Figure 3. 24 SDS PAGE (12%), stained with Coomassie blue, SDS gel shows AFP expression of partially purified pET28-AFP from 200ml culture which was induced by 0.8 mM IPTG at 30 °C for 4 hours. The size of the AFP protein is between 55-70kDa

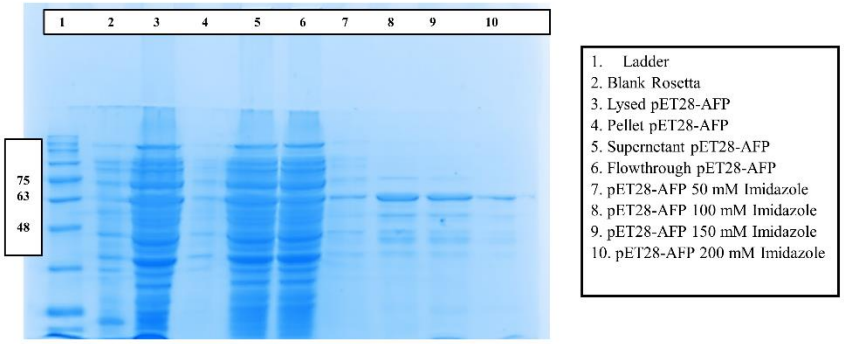

Figure 3. 25 SDS PAGE (12%), stained with Coomassie blue, SDS gel shows AFP expression of partially purified pET28-AFP from 400ml culture which was induced by 0.8 mM IPTG at 30 °C for 4 hours. The size of the AFP protein 63 kDa.

3.3.3. Gel Filtration Chromatography

Gel filtration chromatography results indicated that the recombinant AFP is purified however the concentration of the size excluded recombinant AFP is quite low (Fig 3.26).

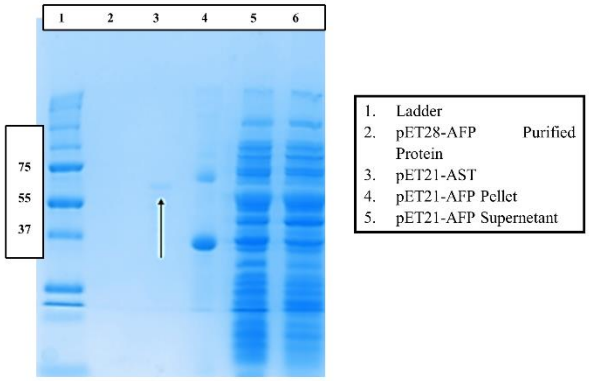

Figure 3. 26 SDS PAGE (12%), stained with Coomassie blue, SDS gel shows AFP expression of purified pET28-AFP from 200ml culture which was induced by 0.5 mM IPTG at 30 °C for 4 hours. The size of the AFP protein is between 55-70kDa. Purified pET28-AFP protein was shown in lane 4.

3.3.4. Protein Concentration Results

Protein concentrations was evaluated by Bradford standard curve as it shown in Figure 3.27. According to the equation given as “y= 0,0017x + 0,0886” the partially purified

recombinant protein concentration was calculated as 8 µg/ml with 0.10 absorbance value at 595 nm.

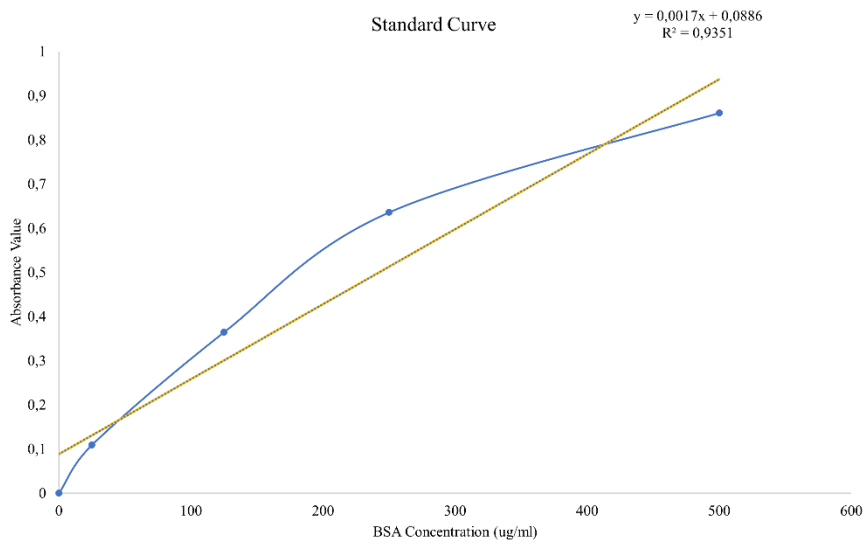

Figure 3. 27 Shows the BSA standard curve obtained by Bradford assay.

3.3.5. Circular Dichroism (CD) Spectroscopy and Thermal Stability Analysis

CD spectroscopy analysis was conducted to analyse the recombinant secondary structure and thermal stability of the recombinant AFP. CD spectrums were collected between -8 °C and 60 °C to determine the effect of temperature change on the recombinant AFP. The CD spectra of the recombinant AFP sample at between 190nm-260 nm indicated the α-helical spectrum with negative bands at 208 nm and 222nm and a positive band at 193 nm (Greenfield, 2006).. The results were indicated that there is no significant structural change up to 40 °C (Fig 4a). Besides, the recombinant AFP showed structural stability even below zero degrees since it demonstrated α-helical spectrum (Fig 4b). Besides, the recombinant AFP showed structural stability even below zero degrees since it demonstrated the α-helical spectrum until -4 °C where the structural distortions were observed.

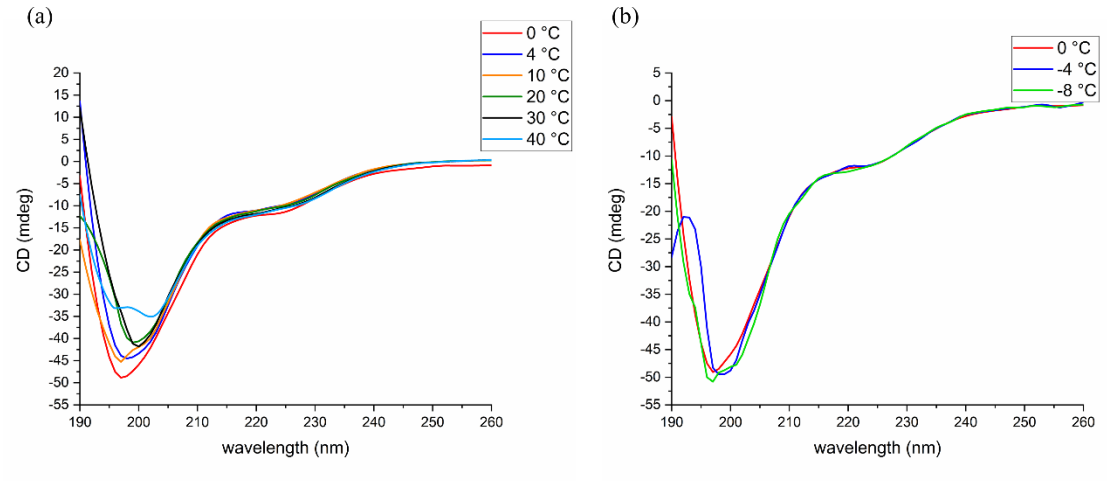

Figure 3. 28. CD spectra of the recombinant AFP, between 190 nm- 260nm a) representation of CD spectrum above 0°C. 0 °C (red), 4 °C (blue), 10 °C (orange), 20 °C (green), 30 °C (black), and 40 °C (navy blue)(b) representation of CD spectrum below 0 °C. 0°C (red), -4 °C (blue), -8 °C (green).

3.3.6. Structure Prediction and homology Modeling

Among the proteins whose structure has been determined AFP from cyanobacterial phycobilisome from *Anabaena sp*. PCC 7120. was found most similar with a homology of 22.7 percent therefore it was used as a template for structure prediction and homology modeling studies, as it was shown in Figure 3.29. Besides, amino acid sequence, general properties and amino acid composition of AFP were presented in table 4 and table 5, respectively.

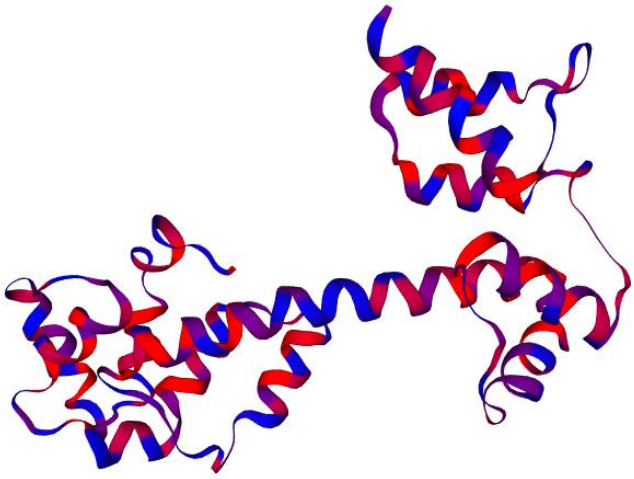

Figure 3. 29. Predicted structure of AFP with %22.7 similarities of Phycobiliprotein ApcE Cryo-EM structure of cyanobacterial phycobilisome from Anabaena sp. PCC 7120.

Table 4. General Properties of AFP

AFP	
Number of amino acids	473
Molecular weight	47316.12 Da
Theoretical pI	3.67
Total number of negatively charged residues (Asp + Glu)	61
Total number of positively charged residues (Arg + Lys)	10
Charge	Negative

Table 5. Amino acid composition of Recombinant AFP

Ala (A) 82	17.3%	Lys (K) 3	0.6 %
Arg (R) 7	1.5%	Met(M) 1	0.2%
Asn(N) 34	7.2%	Phe (F) 14	3.0%
Asp (D) 38	8.0%	Pro (P) 8	1.7%
Cys (C) 0	0.0%	Ser (S) 39	8.2%
Gln (Q) 16	3.4%	Thr (T) 42	8.9%
Glu (E) 23	4.9%	Trp (W) 4	0.8%
Gly (G) 53	11.2%	Tyr (Y) 8	1.7%
His (H) 4	0.8%	Val (V) 35	7.4%
Ile (I) 30	6.3 %	Pyl (O) 0	0.0%
Leu (L) 32	6.8%	Sec (U) 0	0.0%

3.3.7. Anti-icing Activity of the Recombinant AFP coated Aluminium Surfaces

The anti-icing performance of the recombinant AFP coated aluminium surfaces was evaluated by temperature-controlled section of the experimental setup. The tests were conducted while comparing the recombinant AFP coated aluminium surfaces with uncoated aluminium surfaces below zero degrees. The figure 3.30 shows the anti-icing activity of the recombinant AFP immobilized aluminium surfaces and icing formation on

uncoated aluminium surfaces at the surface temperature of -4°C. The results were indicated that, ice crystal growth on the recombinant AFP coated aluminium surfaces is hindered by the recombinant AFP due to the binding of the AFPs to particular interfaces on ice crystals.

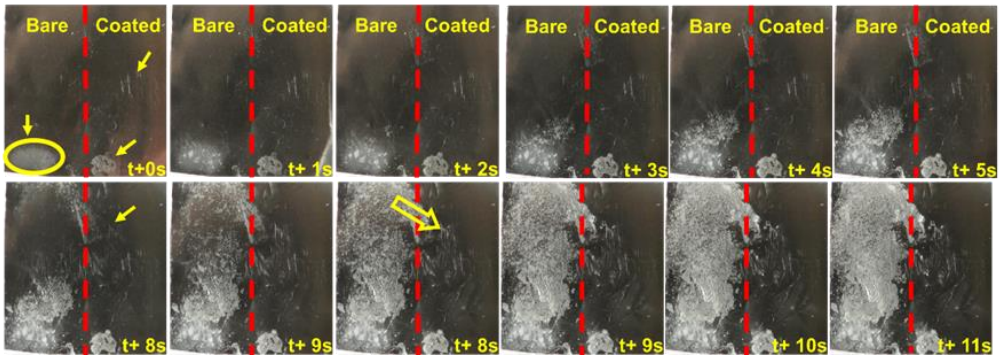

Figure 3. 30 Icing behaviour on the recombinant AFP coated and non-coated aluminium surfaces.

4. DISCUSSION

The present study proposes a synthetic AFP which is utilized for the development of anti-icing surfaces. Ice formation and accumulation on a solid surface can raise severe problems for the heat pumps, solar panels, aircraft, power lines and induces mechanical or electrical malfunctions, increase in energy consumption and safety hazards (Volpe, Gaudiuso, & Ancona, 2020). Several coating agents were employed such as, nano silica (L.-B. Zhang et al., 2023), polysiloxane-modified carbon nanotubes and fluorine-silicone resin(Y. Liu, Shao, Wang, & Wang, 2022), and fluorosilane modified epoxy (Zeng et al., 2021) to obtain anti-icing surfaces. Among them AFPs are favourable due to their safe profile and variety of the IBS according to their structural folding and sequences.

In the current study, the synthetic AFP gene (pUC-AFP) having a same amino acid sequence as original afpA in Mryoi et al. (N. Muryoi et al., 2004) was established by recombinant cloning technology. The original microorganism is the plant growth-promoting rhizobacterium *P. Putida* GR12-2 which is isolated from a soil sample from the Canadian High Arctic. The afpA is expressed by *P. putida* GR12-2 inside a growth medium only under cold temperatures. In the present study, the synthetic AFP was expressed by Rosetta *E. coli* (DE3) cells by the IPTG induction. The SDS PAGE results were indicated that produced AFP has molecular mass of 60 kDa whereas original afpA had 72 kDa size which was even higher from the predicted size, 47.3 kDa. This mass difference could be attributed to the posttranslational modifications (PTMs). PTMs are chemical modifications affecting the protein stability, net charge, binding properties, conformation, and localization (Hashiguchi & Komatsu, 2017; Macek et al., 2019). Several modifications such as, proteolytic cleavage, phosphorylation, glycosylation, methylation, acetylation, lipidation raise PTMs in proteins and alters protein

characteristics such as molecular weight (Larsen, Trelle, Thingholm, & Jensen, 2006; Ramazi & Zahiri, 2021).

The functionality of AFPs is diversified by their ice-binding site (IBS) with the attachments through ice crystal planes. The diversity in amino acid sequence and structure folding of AFPs affects the ice-binding affinity (Khan, Arai, Tsuda, & Kondo, 2021). However, residual variations in the AFPs might have direct relation with antifreeze activity of the AFPs (Wang, Pakhomova, Newcomer, Christner, & Luo, 2017). In the present study, the most repeated residues in the amino acid sequence are Ala (17.3%), Gly (11.2 %), Thr (8.9%), Ser (8.2%), Asp (8%), and Asn (7.2%). The Alanine (Ala) and Threonine (Thr) residues are essential residues in IBS of the AFPs and positioned on the hydrophobic region of the a-helix (Gharib et al., 2022). In a current study, Delesky et al. indicated that Thr polypeptides presented best ice recrystallization inhibition (IRI) activity results among arginine polypeptide and glutamic acid polypeptide (Delesky et al., 2021). Besides, Glycine (Gly) amino acids might have an essential role in the formation of IBS due to having conformationally flexible structure (S. Sun, Ding, Wang, & Han, 2020). An AFP prediction tool, CryoProtect, was developed by Pratiwi et al. (Pratiwi et al., 2017) and indicated that Cysteine (Cys), Serine (Ser), Tryptophan (Trp), Gly, Asparagine (Asn), and Thr were the particular residues of AFPs whereas Leucine (Leu), Valine (Val) , Glutamic Acid (Glu), Isoleucine (Ile) and Methionine (Met) were specific amino acids of non-AFPs (Miyata, Moriwaki, Terada, & Shimizu, 2021). In a recent study, Hudait et al. indicated repeating TxT sequences, where T is Threonine and x is non-conserved amino acid, have strong binding efficiency to ice by anchored clathrate (AC) motifs (Hudait, Qiu, Odendahl, & Molinero, 2019). The clathrate-like waters are formed around the methyl groups of the Thr residues by water molecules in the AC motifs and bound hydroxyl group of the proteins. Hydrophobicity of the AFPs is another essential factor that influences ordering of water molecules while ice formation since IBSs of the AFPs are relatively hydrophobic (Davies, 2014; Hanada, Nishimiya, Miura, Tsuda, & Kondo, 2014). In the present study, the synthetic AFP could be indicated as an effective AFP due to the abundance of Ala, Gly, and Thr residues, having 4 TxT repeated sequences (Fig 3.32) and hydrophobic characteristics in the whole sequence which demonstrates the functional IBS of the AFP (Fig 3.31).

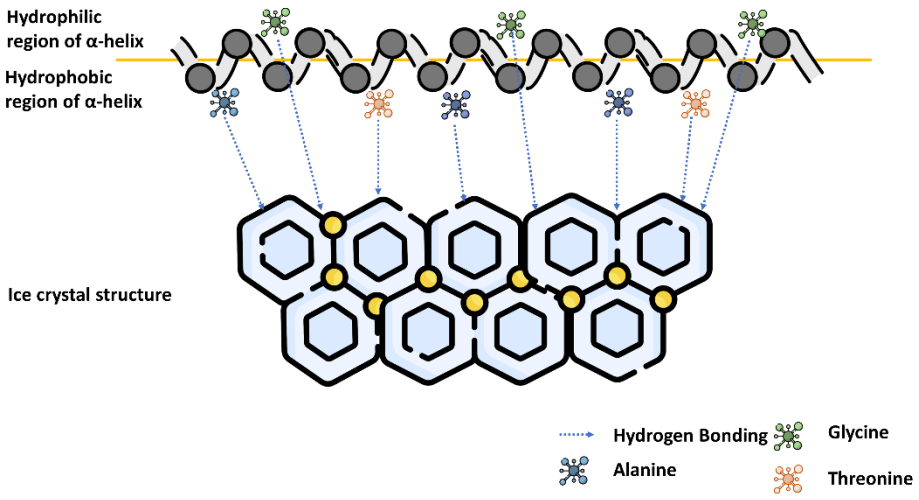

Figure 4. 1 Schematic represents for ice binding of threonine (orange), glycine (green), alanine (blue) residues to the ice crystals by hydrogen bonding.

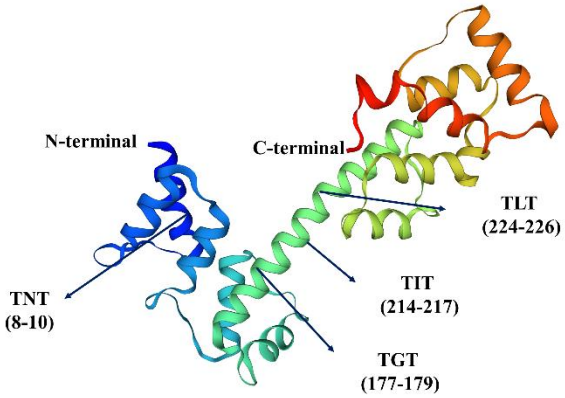

Figure 4. 2 The predicted 3D structure of the recombinant AFP showing TxT repeating units.

5. CONCLUSION

This thesis study presents the production of AFP using the recombinant technology, following by its novel immobilization on metallic surfaces and further demonstration of anti-icing activity. The major aim is to propose an environmentally friendly coating and to show its applicability to relevant industries such as refrigeration systems. The recombinant technology enables the large-scale protein production of the AFP for industrial applications via surface immobilization methods. The application of oxygen plasma allows activation of surface functional groups on surfaces and suitable for different shapes and geometries while increasing coating stability. In the current study, produced recombinant AFP was coated on aluminium surfaces with oxygen plasma pre-treatment and the activity of AFP-immobilized surfaces were tested at different conditions. It is demonstrated that the developed AFP-coated surfaces delay the ice formation and can prevent ice nucleation and growth. Consequently, this study offers a new perspective for biotechnological applications of antifreeze proteins to ensure energy-saving purposes with an environmentally friendly aspect. For further studies, the effect of different coating substrates on the anti-icing activity of the recombinant AFP and different coating methods to increase the stability of the recombinant protein on surfaces can be investigated.

6. REFERENCES

Al-Tubuly, A. A. (2000). SDS-PAGE and Western Blotting. *Methods Mol Med, 40*, 391-405. doi:10.1385/1-59259-076-4:391

Arai, T., Yamauchi, A., Miura, A., Kondo, H., Nishimiya, Y., Sasaki, Y. C., & Tsuda, S. (2021). Discovery of Hyperactive Antifreeze Protein from Phylogenetically Distant Beetles Questions Its Evolutionary Origin. *22*(7), 3637.

Arcarons, N., Vendrell-Flotats, M., Yeste, M., Mercade, E., López-Béjar, M., & Mogas, T. (2019). Cryoprotectant role of exopolysaccharide of Pseudomonas sp. ID1 in the vitrification of IVM cow oocytes %J Reproduction, Fertility and Development. *31*(9), 1507-1519. doi:https://doi.org/10.1071/RD18447

Baguisi, A., Arav, A., Crosby, T. F., Roche, J. F., & Boland, M. P. (1997). Hypothermic storage of sheep embryos with antifreeze proteins: Development in vitro and in vivo. *Theriogenology, 48*(6), 1017-1024. doi:https://doi.org/10.1016/S0093-691X(97)00328-2

Balamurugan, S., Ann, J. S., Varghese, I. P., Murugan, S. B., Harish, M. C., Kumar, S. R., & Sathishkumar, R. (2018). Heterologous expression of Lolium perenne antifreeze protein confers chilling tolerance in tomato. *Journal of Integrative Agriculture, 17*(5), 1128-1136. doi:https://doi.org/10.1016/S2095-3119(17)61735-0

Baskaran, A., Kaari, M., Venugopal, G., Manikkam, R., Joseph, J., & Bhaskar, P. V. (2021). Anti freeze proteins (Afp): Properties, sources and applications – A review. *International Journal of Biological Macromolecules, 189*, 292-305. doi:https://doi.org/10.1016/j.ijbiomac.2021.08.105

Baust, J. G., Corwin, W. L., & Baust, J. M. (2011). 1.12 - Cell Preservation Technology. In M. Moo-Young (Ed.), *Comprehensive Biotechnology (Third Edition)* (pp. 154-165). Oxford: Pergamon.

Bayer-Giraldi, M., Uhlig, C., John, U., Mock, T., & Valentin, K. (2010). Antifreeze proteins in polar sea ice diatoms: diversity and gene expression in the genus Fragilariopsis. *12*(4), 1041-1052. doi:https://doi.org/10.1111/j.1462-2920.2009.02149.x

Beirão, J., Zilli, L., Vilella, S., Cabrita, E., Schiavone, R., & Herráez, M. P. (2012). Improving Sperm Cryopreservation with Antifreeze Proteins: Effect on Gilthead Seabream (Sparus aurata) Plasma Membrane Lipids1. *Biology of Reproduction, 86*(2). doi:10.1095/biolreprod.111.093401

Best, B. P. (2015). Cryoprotectant Toxicity: Facts, Issues, and Questions. *Rejuvenation Res, 18*(5), 422-436. doi:10.1089/rej.2014.1656

Białkowska, A., Majewska, E., Olczak, A., & Twarda-Clapa, A. (2020). Ice Binding Proteins: Diverse Biological Roles and Applications in Different Types of Industry. *Biomolecules, 10*(2). doi:10.3390/biom10020274

Boonsupthip, W., & Lee, T.-C. (2003). Application of Antifreeze Protein for Food Preservation: Effect of Type III Antifreeze Protein for Preservation of Gel-forming of Frozen and Chilled Actomyosin. *68*(5), 1804-1809. doi:https://doi.org/10.1111/j.1365-2621.2003.tb12333.x

Bredow, M., & Walker, V. K. (2017). Ice-Binding Proteins in Plants. *Frontiers in Plant Science, 8*. doi:10.3389/fpls.2017.02153

Collins, T., & Margesin, R. (2019). Psychrophilic lifestyles: mechanisms of adaptation and biotechnological tools. *Applied Microbiology and Biotechnology, 103*(7), 2857-2871. doi:10.1007/s00253-019-09659-5

Davies, P. L. (2014). Ice-binding proteins: a remarkable diversity of structures for stopping and starting ice growth. *Trends in Biochemical Sciences, 39*(11), 548-555. doi:https://doi.org/10.1016/j.tibs.2014.09.005

Davies, P. L., & Sykes, B. D. (1997). Antifreeze proteins. *Current Opinion in Structural Biology, 7*(6), 828-834. doi:https://doi.org/10.1016/S0959-440X(97)80154-6

De Geyter, N., & Morent, R. (2014). 7 - Cold plasma surface modification of biodegradable polymer biomaterials. In P. Dubruel & S. Van Vlierberghe (Eds.), *Biomaterials for Bone Regeneration* (pp. 202-224): Woodhead Publishing.

Delesky, E. A., García, L. M., Lobo, A. J., Wallat, J. D., Miyake, G. M., & Srubar III, W. V. (2021). A Bioinspired Threonine-based Antifreeze Protein Mimic with Potent Ice Recrystallization Inhibition Activity. *ChemRxiv*.

DeVries, A. L., & Wohlschlag, D. E. (1969). Freezing resistance in some Antarctic fishes. *Science, 163*(3871), 1073-1075. doi:10.1126/science.163.3871.1073

Donovan, R. S., Robinson, C. W., & Glick, B. R. (1996). Review: optimizing inducer and culture conditions for expression of foreign proteins under the control of the lac promoter. *J Ind Microbiol, 16*(3), 145-154. doi:10.1007/bf01569997

Duman, J. G. (2015). Animal ice-binding (antifreeze) proteins and glycolipids: an overview with emphasis on physiological function. *Journal of Experimental Biology, 218*(12), 1846-1855. doi:10.1242/jeb.116905

Duman, J. G., Bennett, V., Sformo, T., Hochstrasser, R., & Barnes, B. M. (2004). Antifreeze proteins in Alaskan insects and spiders. *Journal of Insect Physiology, 50*(4), 259-266. doi:https://doi.org/10.1016/j.jinsphys.2003.12.003

Duman, J. G., & Newton, S. S. (2020). Antifreeze Proteins in Other Species. In H. Ramløv & D. S. Friis (Eds.), *Antifreeze Proteins Volume 1: Environment, Systematics and Evolution* (pp. 227-273). Cham: Springer International Publishing.

Ekpo, M. D., Xie, J., Hu, Y., Liu, X., Liu, F., Xiang, J., . . . Tan, S. (2022). Antifreeze Proteins: Novel Applications and Navigation towards Their Clinical Application in Cryobanking. *23*(5), 2639.

Eskandari, A., Leow, T. C., Rahman, M. B. A., & Oslan, S. N. (2020). Antifreeze Proteins and Their Practical Utilization in Industry, Medicine, and Agriculture. *Biomolecules, 10*(12). doi:10.3390/biom10121649

Esser-Kahn, A. P., Trang, V., & Francis, M. B. (2010). Incorporation of Antifreeze Proteins into Polymer Coatings Using Site-Selective Bioconjugation. *Journal of the American Chemical Society, 132*(38), 13264-13269. doi:10.1021/ja103038p

Garnham, C. P., Natarajan, A., Middleton, A. J., Kuiper, M. J., Braslavsky, I., & Davies, P. L. (2010). Compound ice-binding site of an antifreeze protein revealed by mutagenesis and fluorescent tagging. *Biochemistry, 49*(42), 9063-9071.

Ghannam, M. G., & Varacallo, M. (2018). Biochemistry, Polymerase Chain Reaction.

Gharib, G., Saeidiharzand, S., Sadaghiani, A. K., & Koşar, A. (2022). Antifreeze Proteins: A Tale of Evolution From Origin to Energy Applications. *Frontiers in Bioengineering and Biotechnology, 9*. doi:10.3389/fbioe.2021.770588

Graether, S. P., Kuiper, M. J., Gagné, S. M., Walker, V. K., Jia, Z., Sykes, B. D., & Davies, P. L. (2000). β-Helix structure and ice-binding properties of a hyperactive antifreeze protein from an insect. *Nature, 406*(6793), 325-328. doi:10.1038/35018610

Greenfield, N. J. (2006). Using circular dichroism spectra to estimate protein secondary structure. *Nature Protocols, 1*(6), 2876-2890. doi:10.1038/nprot.2006.202

Gupta, R., & Deswal, R. (2012). Low Temperature Stress Modulated Secretome Analysis and Purification of Antifreeze Protein from Hippophae rhamnoides, a Himalayan Wonder Plant. *Journal of Proteome Research, 11*(5), 2684-2696. doi:10.1021/pr200944z

Gupta, R., & Deswal, R. (2014). Antifreeze proteins enable plants to survive in freezing conditions. *J Biosci, 39*(5), 931-944. doi:10.1007/s12038-014-9468-2

Gupta, R., & Deswal, R. (2014). Antifreeze proteins enable plants to survive in freezing conditions. *J Biosci, 39*(5), 931-944. doi:10.1007/s12038-014-9468-2

Gwak, I. G., sic Jung, W., Kim, H. J., Kang, S.-H., & Jin, E. (2010). Antifreeze Protein in Antarctic Marine Diatom, Chaetoceros neogracile. *Marine Biotechnology, 12*(6), 630-639. doi:10.1007/s10126-009-9250-x

Gwak, Y., Park, J.-i., Kim, M., Kim, H. S., Kwon, M. J., Oh, S. J., . . . Jin, E. (2015). Creating Anti-icing Surfaces via the Direct Immobilization of Antifreeze Proteins on Aluminum. *Scientific Reports, 5*(1), 12019. doi:10.1038/srep12019

Hanada, Y., Nishimiya, Y., Miura, A., Tsuda, S., & Kondo, H. (2014). Hyperactive antifreeze protein from an Antarctic sea ice bacterium Colwellia sp. has a compound ice-binding site without repetitive sequences. *The FEBS Journal, 281*(16), 3576-3590. doi:https://doi.org/10.1111/febs.12878

Hashiguchi, A., & Komatsu, S. (2017). Chapter Six - Posttranslational Modifications and Plant–Environment Interaction. In A. K. Shukla (Ed.), *Methods in Enzymology* (Vol. 586, pp. 97-113): Academic Press.

Hashim, N. H. F., Bharudin, I., Nguong, D. L. S., Higa, S., Bakar, F. D. A., Nathan, S., . . . Murad, A. M. A. (2013). Characterization of Afp1, an antifreeze protein from the psychrophilic yeast Glaciozymaantarctica PI12. *Extremophiles, 17*(1), 63-73. doi:10.1007/s00792-012-0494-4

Hirano, Y., Nishimiya, Y., Matsumoto, S., Matsushita, M., Todo, S., Miura, A., . . . Tsuda, S. (2008). Hypothermic preservation effect on mammalian cells of type III antifreeze proteins from notched-fin eelpout. *Cryobiology, 57*(1), 46-51. doi:https://doi.org/10.1016/j.cryobiol.2008.05.006

Hon, W. C., Griffith, M., Mlynarz, A., Kwok, Y. C., & Yang, D. (1995). Antifreeze Proteins in Winter Rye Are Similar to Pathogenesis-Related Proteins. *Plant Physiology, 109*(3), 879-889. doi:10.1104/pp.109.3.879 %J Plant Physiology

How to Perform DNA Electrophoresis in Agarose Gel？. (2022). Retrieved from https://www.gelepchina.com/news/how-to-perform-dna-electrophoresis-in-agarose-gel%EF%BC%9F/

Hu, P. F., Li, X. C., Lei, N., Lan, X. Y., Zhao, Q. J., Guan, W. J., & Ma, Y. H. (2013). Study on characteristics of chemokine CXCL10 gene cloned from cDNA expression library of Ujumqin sheep. *Biomed Res Int, 2013*, 217942. doi:10.1155/2013/217942

Hudait, A., Qiu, Y., Odendahl, N., & Molinero, V. (2019). Hydrogen-Bonding and Hydrophobic Groups Contribute Equally to the Binding of Hyperactive Antifreeze and Ice-Nucleating Proteins to Ice. *Journal of the American Chemical Society, 141*(19), 7887-7898. doi:10.1021/jacs.9b02248

Jeong, Y., Jeong, S., Nam, Y. K., & Kang, S. M. (2018). Development of Freeze-resistant Aluminum Surfaces by Tannic Acid Coating and Subsequent Immobilization of Antifreeze Proteins. *Bulletin of the Korean Chemical Society, 39*(4), 559-562. doi:https://doi.org/10.1002/bkcs.11406

Kaleda, A., Tsanev, R., Klesment, T., Vilu, R., & Laos, K. (2018). Ice cream structure modification by ice-binding proteins. *Food Chemistry, 246*, 164-171. doi:https://doi.org/10.1016/j.foodchem.2017.10.152

Kaushik, J. K., & Bhat, R. (2003). Why Is Trehalose an Exceptional Protein Stabilizer?: AN ANALYSIS OF THE THERMAL STABILITY OF PROTEINS IN THE PRESENCE OF THE COMPATIBLE OSMOLYTE TREHALOSE*. *Journal of Biological Chemistry, 278*(29), 26458-26465. doi:https://doi.org/10.1074/jbc.M300815200

Kawahara, H., Nakano, Y., Omiya, K., Muryoi, N., Nishikawa, J., & Obata, H. (2004). Production of two types of ice crystal-controlling proteins in Antarctic bacterium. *Journal of Bioscience and Bioengineering, 98*(3), 220-223. doi:https://doi.org/10.1016/S1389-1723(04)00271-3

Khan, N. M. M. U., Arai, T., Tsuda, S., & Kondo, H. (2021). Characterization of microbial antifreeze protein with intermediate activity suggests that a bound-water network is essential for hyperactivity. *Scientific Reports, 11*(1), 5971. doi:10.1038/s41598-021-85559-x

Khanna, H. K., & Daggard, G. E. (2006). Targeted expression of redesigned and codon optimised synthetic gene leads to recrystallisation inhibition and reduced electrolyte leakage in spring wheat at sub-zero temperatures. *Plant Cell Reports, 25*(12), 1336-1346. doi:10.1007/s00299-006-0191-9

Kim, H. J., Lee, J. H., Hur, Y. B., Lee, C. W., Park, S.-H., & Koo, B.-W. (2017). Marine Antifreeze Proteins: Structure, Function, and Application to Cryopreservation as a Potential Cryoprotectant. *15*(2), 27.

Kim, H. J., Lee, J. H., Hur, Y. B., Lee, C. W., Park, S. H., & Koo, B. W. (2017). Marine Antifreeze Proteins: Structure, Function, and Application to Cryopreservation as a Potential Cryoprotectant. *Mar Drugs, 15*(2). doi:10.3390/md15020027

Knight, C. A., Cheng, C. C., & DeVries, A. L. (1991). Adsorption of alpha-helical antifreeze peptides on specific ice crystal surface planes. *Biophysical Journal, 59*(2), 409-418. doi:https://doi.org/10.1016/S0006-3495(91)82234-2

Koshio, K., Arai, K., Waku, T., Wilson, P. W., & Hagiwara, Y. (2018). Suppression of droplets freezing on glass surfaces on which antifreeze polypeptides are adhered by a silane coupling agent. *PLOS ONE, 13*(10), e0204686. doi:10.1371/journal.pone.0204686

Laemmli, U. K. (1970). Cleavage of structural proteins during the assembly of the head of bacteriophage T4. *Nature, 227*(5259), 680-685.

Larsen, M. R., Trelle, M. B., Thingholm, T. E., & Jensen, O. N. (2006). Analysis of posttranslational modifications of proteins by tandem mass spectrometry. *40*(6), 790-798. doi:10.2144/000112201

Lee, E. K., & Koros, W. J. (2003). Membranes, Synthetic, Applications. In R. A. Meyers (Ed.), *Encyclopedia of Physical Science and Technology (Third Edition)* (pp. 279-344). New York: Academic Press.

Lee, H. H., Lee, H. J., Kim, H. J., Lee, J. H., Ko, Y., Kim, S. M., . . . Kim, S. H. (2015). Effects of antifreeze proteins on the vitrification of mouse oocytes: comparison of three different antifreeze proteins. *Hum Reprod, 30*(9), 2110-2119. doi:10.1093/humrep/dev170

Lee, J. K., & Kim, H. J. (2016). Cloning, expression, and activity of type IV antifreeze protein from cultured subtropical olive flounder (Paralichthys olivaceus). *Fisheries and Aquatic Sciences, 19*(1), 33. doi:10.1186/s41240-016-0033-9

Lee, J. K., Park, K. S., Park, S., Park, H., Song, Y. H., Kang, S.-H., & Kim, H. J. (2010). An extracellular ice-binding glycoprotein from an Arctic psychrophilic yeast. *Cryobiology, 60*(2), 222-228. doi:https://doi.org/10.1016/j.cryobiol.2010.01.002

Lee, P. Y., Costumbrado, J., Hsu, C. Y., & Kim, Y. H. (2012). Agarose gel electrophoresis for the separation of DNA fragments. *J Vis Exp*(62). doi:10.3791/3923

Liang, S., Yuan, B., Kwon, J.-W., Ahn, M., Cui, X.-S., Bang, J. K., & Kim, N.-H. (2016). Effect of antifreeze glycoprotein 8 supplementation during vitrification on the developmental competence of bovine oocytes. *Theriogenology, 86*(2), 485-494.e481. doi:https://doi.org/10.1016/j.theriogenology.2016.01.032

Lin, F.-H., Davies, P. L., & Graham, L. A. (2011). The Thr- and Ala-Rich Hyperactive Antifreeze Protein from Inchworm Folds as a Flat Silk-like β-Helix. *Biochemistry, 50*(21), 4467-4478. doi:10.1021/bi2003108

Liu, K., Wang, C., Ma, J., Shi, G., Yao, X., Fang, H., . . . Wang, J. (2016). Janus effect of antifreeze proteins on ice nucleation. *Proceedings of the National Academy of Sciences, 113*(51), 14739-14744. doi:doi:10.1073/pnas.1614379114

Liu, M., Liang, Y., Zhang, H., Wu, G., Wang, L., Qian, H., & Qi, X. (2018). Comparative Study on the Cryoprotective Effects of Three Recombinant Antifreeze Proteins from Pichia

pastoris GS115 on Hydrated Gluten Proteins during Freezing. *Journal of Agricultural and Food Chemistry, 66*(24), 6151-6161. doi:10.1021/acs.jafc.8b00910
Liu, Y., Shao, Y., Wang, Y., & Wang, J. (2022). An abrasion-resistant, photothermal, superhydrophobic anti-icing coating prepared by polysiloxane-modified carbon nanotubes and fluorine-silicone resin. *Colloids and Surfaces A: Physicochemical and Engineering Aspects, 648*, 129335. doi:https://doi.org/10.1016/j.colsurfa.2022.129335
Lopez Ortiz, J. I., Quiroga, E., Narambuena, C. F., Riccardo, J. L., & Ramirez-Pastor, A. J. (2021). Thermal hysteresis activity of antifreeze proteins: A model based on fractional statistics theory of adsorption. *Physica A: Statistical Mechanics and its Applications, 575*, 126046. doi:https://doi.org/10.1016/j.physa.2021.126046
Macek, B., Forchhammer, K., Hardouin, J., Weber-Ban, E., Grangeasse, C., & Mijakovic, I. (2019). Protein post-translational modifications in bacteria. *Nature Reviews Microbiology, 17*(11), 651-664. doi:10.1038/s41579-019-0243-0
Mangiagalli, M., Bar-Dolev, M., Tedesco, P., Natalello, A., Kaleda, A., Brocca, S., . . . Lotti, M. (2017). Cryo-protective effect of an ice-binding protein derived from Antarctic bacteria. *284*(1), 163-177. doi:https://doi.org/10.1111/febs.13965
Marshall, C. B., Chakrabartty, A., & Davies, P. L. (2005). Hyperactive Antifreeze Protein from Winter Flounder Is a Very Long Rod-like Dimer of α-Helices*. *Journal of Biological Chemistry, 280*(18), 17920-17929. doi:https://doi.org/10.1074/jbc.M500622200
Martínez-Páramo, S., Barbosa, V., Pérez-Cerezales, S., Robles, V., & Herráez, M. P. (2009). Cryoprotective effects of antifreeze proteins delivered into zebrafish embryos. *Cryobiology, 58*(2), 128-133. doi:https://doi.org/10.1016/j.cryobiol.2008.11.013
Martínez-Páramo, S., Pérez-Cerezales, S., Robles, V., Anel, L., & Herráez, M. P. (2008). Incorporation of antifreeze proteins into zebrafish embryos by a non-invasive method. *Cryobiology, 56*(3), 216-222. doi:10.1016/j.cryobiol.2008.03.003
Mazorra-Manzano, M. A., Ramírez-Suárez, J. C., Moreno-Hernández, J. M., & Pacheco-Aguilar, R. (2018). 17 - Seafood proteins. In R. Y. Yada (Ed.), *Proteins in Food Processing (Second Edition)* (pp. 445-475): Woodhead Publishing.
Meister, K., Ebbinghaus, S., Xu, Y., Duman, J. G., DeVries, A., Gruebele, M., . . . Havenith, M. (2013a). Long-range protein–water dynamics in hyperactive insect antifreeze proteins. *Proceedings of the National Academy of Sciences, 110*(5), 1617-1622. doi:10.1073/pnas.1214911110
Meister, K., Ebbinghaus, S., Xu, Y., Duman, J. G., DeVries, A., Gruebele, M., . . . Havenith, M. (2013b). Long-range protein–water dynamics in hyperactive insect antifreeze proteins. *110*(5), 1617-1622. doi:doi:10.1073/pnas.1214911110
Miyata, R., Moriwaki, Y., Terada, T., & Shimizu, K. (2021). Prediction and analysis of antifreeze proteins. *Heliyon, 7*(9), e07953. doi:10.1016/j.heliyon.2021.e07953
Muryoi, N., Sato, M., Kaneko, S., Kawahara, H., Obata, H., Yaish, M. W., . . . Glick, B. R. (2004). Cloning and expression of afpA, a gene encoding an antifreeze protein from the arctic plant growth-promoting rhizobacterium Pseudomonas putida GR12-2. *J Bacteriol, 186*(17), 5661-5671. doi:10.1128/jb.186.17.5661-5671.2004
Muryoi, N., Sato, M., Kaneko, S., Kawahara, H., Obata, H., Yaish, M. W. F., . . . Glick, B. R. (2004). Cloning and Expression of afpA, a Gene Encoding an Antifreeze Protein from the Arctic Plant Growth-Promoting Rhizobacterium Pseudomonas putida GR12-2. *186*(17), 5661-5671. doi:doi:10.1128/JB.186.17.5661-5671.2004
Naing, A. H., & Kim, C. K. (2019). A brief review of applications of antifreeze proteins in cryopreservation and metabolic genetic engineering. *3 Biotech, 9*(9), 329. doi:10.1007/s13205-019-1861-y
Nishijima, K., Tanaka, M., Sakai, Y., Koshimoto, C., Morimoto, M., Watanabe, T., . . . Kitajima, S. (2014). Effects of type III antifreeze protein on sperm and embryo cryopreservation in rabbit. *Cryobiology, 69*(1), 22-25. doi:10.1016/j.cryobiol.2014.04.014

Nishijima, K., Tanaka, M., Sakai, Y., Koshimoto, C., Morimoto, M., Watanabe, T., . . . Kitajima, S. (2014). Effects of type III antifreeze protein on sperm and embryo cryopreservation in rabbit. *Cryobiology, 69*(1), 22-25. doi:https://doi.org/10.1016/j.cryobiol.2014.04.014

Nishimiya, Y., Kondo, H., Takamichi, M., Sugimoto, H., Suzuki, M., Miura, A., & Tsuda, S. (2008). Crystal Structure and Mutational Analysis of Ca2+-Independent Type II Antifreeze Protein from Longsnout Poacher, Brachyopsis rostratus. *Journal of Molecular Biology, 382*(3), 734-746. doi:https://doi.org/10.1016/j.jmb.2008.07.042

Olijve, L. L. C., Meister, K., DeVries, A. L., Duman, J. G., Guo, S., Bakker, H. J., & Voets, I. K. (2016a). Blocking rapid ice crystal growth through nonbasal plane adsorption of antifreeze proteins. *Proceedings of the National Academy of Sciences, 113*(14), 3740-3745. doi:doi:10.1073/pnas.1524109113

Olijve, L. L. C., Meister, K., DeVries, A. L., Duman, J. G., Guo, S., Bakker, H. J., & Voets, I. K. (2016b). Blocking rapid ice crystal growth through nonbasal plane adsorption of antifreeze proteins. *113*(14), 3740-3745. doi:doi:10.1073/pnas.1524109113

Osborne, R. (2015).

Prapulla, S. G., & Karanth, N. G. (2014). FERMENTATION (INDUSTRIAL) | Recovery of Metabolites. In C. A. Batt & M. L. Tortorello (Eds.), *Encyclopedia of Food Microbiology (Second Edition)* (pp. 822-833). Oxford: Academic Press.

Pratiwi, R., Malik, A. A., Schaduangrat, N., Prachayasittikul, V., Wikberg, J. E. S., Nantasenamat, C., & Shoombuatong, W. (2017). CryoProtect: A Web Server for Classifying Antifreeze Proteins from Nonantifreeze Proteins. *Journal of Chemistry, 2017*, 9861752. doi:10.1155/2017/9861752

Rahman, A. T., Arai, T., Yamauchi, A., Miura, A., Kondo, H., Ohyama, Y., & Tsuda, S. (2019). Ice recrystallization is strongly inhibited when antifreeze proteins bind to multiple ice planes. *Scientific Reports, 9*(1), 2212. doi:10.1038/s41598-018-36546-2

Ramazi, S., & Zahiri, J. (2021). Post-translational modifications in proteins: resources, tools and prediction methods. *Database, 2021*, baab012. doi:10.1093/database/baab012

Sambrook, J., Fritsch, E. F., & Maniatis, T. (1989). *Molecular cloning: a laboratory manual*: Cold spring harbor laboratory press.

Shehadul Islam, M., Aryasomayajula, A., & Selvaganapathy, P. R. *A Review on Macroscale and Microscale Cell Lysis Methods*: Micromachines (Basel). 2017 Mar 8;8(3):83. doi: 10.3390/mi8030083. eCollection 2017 Mar.

Smolin, N., & Daggett, V. (2008). Formation of Ice-like Water Structure on the Surface of an Antifreeze Protein. *The Journal of Physical Chemistry B, 112*(19), 6193-6202. doi:10.1021/jp710546e

Sun, S., Ding, H., Wang, D., & Han, S. (2020). Identifying Antifreeze Proteins Based on Key Evolutionary Information. *Frontiers in Bioengineering and Biotechnology, 8*. doi:10.3389/fbioe.2020.00244

Sun, W.-S., Jang, H., Kwon, H. J., Kim, K. Y., Ahn, S. B., Hwang, S., . . . Lee, J.-W. (2020). The protective effect of Leucosporidium-derived ice-binding protein (LeIBP) on bovine oocytes and embryos during vitrification. *Theriogenology, 151*, 137-143. doi:https://doi.org/10.1016/j.theriogenology.2020.04.016

Sun, X., Griffith, M., Pasternak, J. J., & Glick, B. R. (1995a). Low temperature growth, freezing survival, and production of antifreeze protein by the plant growth promoting rhizobacterium Pseudomonas putida GR12-2. *Canadian Journal of Microbiology, 41*(9), 776-784. doi:10.1139/m95-107 %M 7585354

Sun, X., Griffith, M., Pasternak, J. J., & Glick, B. R. (1995b). Low temperature growth, freezing survival, and production of antifreeze protein by the plant growth promoting rhizobacterium Pseudomonas putida GR12-2. *41*(9), 776-784. doi:10.1139/m95-107 %M 7585354

Sutariya, S. G., & Sunkesula, V. (2021). 3.03 - Food Freezing: Emerging Techniques for Improving Quality and Process Efficiency a Comprehensive Review. In K. Knoerzer & K.

Muthukumarappan (Eds.), *Innovative Food Processing Technologies* (pp. 36-63). Oxford: Elsevier.
Tahergorabi, R., Hosseini, S. V., & Jaczynski, J. (2011). 6 - Seafood proteins. In G. O. Phillips & P. A. Williams (Eds.), *Handbook of Food Proteins* (pp. 116-149): Woodhead Publishing.
Tejo, B. A., Asmawi, A. A., & Rahman, M. B. A. (2020). Antifreeze proteins: characteristics and potential applications. *Makara Journal of Science, 24*(1), 8.
Tian, Y., Zhu, Z., & Sun, D.-W. (2020). Naturally sourced biosubstances for regulating freezing points in food researches: Fundamentals, current applications and future trends. *Trends in Food Science & Technology, 95*, 131-140. doi:https://doi.org/10.1016/j.tifs.2019.11.009
Vance, T. D. R., Bayer-Giraldi, M., Davies, P. L., & Mangiagalli, M. (2019). Ice-binding proteins and the 'domain of unknown function' 3494 family. *286*(5), 855-873. doi:https://doi.org/10.1111/febs.14764
Volpe, A., Gaudiuso, C., & Ancona, A. (2020). Laser Fabrication of Anti-Icing Surfaces: A Review. *Materials, 13*(24), 5692.
Wallis, J. G., Wang, H., & Guerra*, D. J. (1997). Expression of a synthetic antifreeze protein in potato reduces electrolyte release at freezing temperatures. *Plant Molecular Biology, 35*(3), 323-330. doi:10.1023/A:1005886210159
Wang, C., Pakhomova, S., Newcomer, M. E., Christner, B. C., & Luo, B. H. (2017). Structural basis of antifreeze activity of a bacterial multi-domain antifreeze protein. *PLoS One, 12*(11), e0187169. doi:10.1371/journal.pone.0187169
Wen, D., & Laursen, R. A. (1992). A model for binding of an antifreeze polypeptide to ice. *Biophysical Journal, 63*(6), 1659-1662. doi:https://doi.org/10.1016/S0006-3495(92)81750-2
Wierzbicki, A., Madura, J. D., Salmon, C., & Sönnichsen, F. (1997). Modeling studies of binding of sea raven type II antifreeze protein to ice. *Journal of chemical information and computer sciences, 37*(6), 1006-1010.
Xiang, H., Yang, X., Ke, L., & Hu, Y. (2020). The properties, biotechnologies, and applications of antifreeze proteins. *International Journal of Biological Macromolecules, 153*, 661-675. doi:https://doi.org/10.1016/j.ijbiomac.2020.03.040
Xu, H., Griffith, M., Patten, C. L., & Glick, B. R. (1998). Isolation and characterization of an antifreeze protein with ice nucleation activity from the plant growth promoting rhizobacterium Pseudomonas putida GR12-2. *44*(1), 64-73. doi:10.1139/w97-126
YAMASHITA, Y., NAKAMURA, N., OMIYA, K., NISHIKAWA, J., KAWAHARA, H., & OBATA, H. (2002). Identification of an Antifreeze Lipoprotein from Moraxella sp. of Antarctic Origin. *Bioscience, Biotechnology, and Biochemistry, 66*(2), 239-247. doi:10.1271/bbb.66.239 %J Bioscience, Biotechnology, and Biochemistry
Yeh, C.-M., Kao, B.-Y., & Peng, H.-J. (2009). Production of a Recombinant Type 1 Antifreeze Protein Analogue by L. lactis and Its Applications on Frozen Meat and Frozen Dough. *Journal of Agricultural and Food Chemistry, 57*(14), 6216-6223. doi:10.1021/jf900924f
Yu, S. O., Brown, A., Middleton, A. J., Tomczak, M. M., Walker, V. K., & Davies, P. L. (2010). Ice restructuring inhibition activities in antifreeze proteins with distinct differences in thermal hysteresis. *Cryobiology, 61*(3), 327-334. doi:https://doi.org/10.1016/j.cryobiol.2010.10.158
Zeng, D., Li, Y., Huan, D., Liu, H., Luo, H., Cui, Y., . . . Wang, J. (2021). Robust epoxy-modified superhydrophobic coating for aircraft anti-icing systems. *Colloids and Surfaces A: Physicochemical and Engineering Aspects, 628*, 127377. doi:https://doi.org/10.1016/j.colsurfa.2021.127377
Zhang, D.-Q., Liu, B., Feng, D.-R., He, Y.-M., & Wang, J.-F. (2004). Expression, purification, and antifreeze activity of carrot antifreeze protein and its mutants. *Protein Expression and Purification, 35*(2), 257-263. doi:https://doi.org/10.1016/j.pep.2004.01.019

Zhang, L.-B., Zhang, H.-X., Liu, Z.-J., Jiang, X.-Y., Agathopoulos, S., Deng, Z., . . . Yin, L.-J. (2023). Nano-silica anti-icing coatings for protecting wind-power turbine fan blades. *Journal of Colloid and Interface Science, 630*, 1-10. doi:https://doi.org/10.1016/j.jcis.2022.09.154

APPENDIX

APPENDIX 1- Sequence Analysis Results for pET$_{28}$-AFP (Promoter)

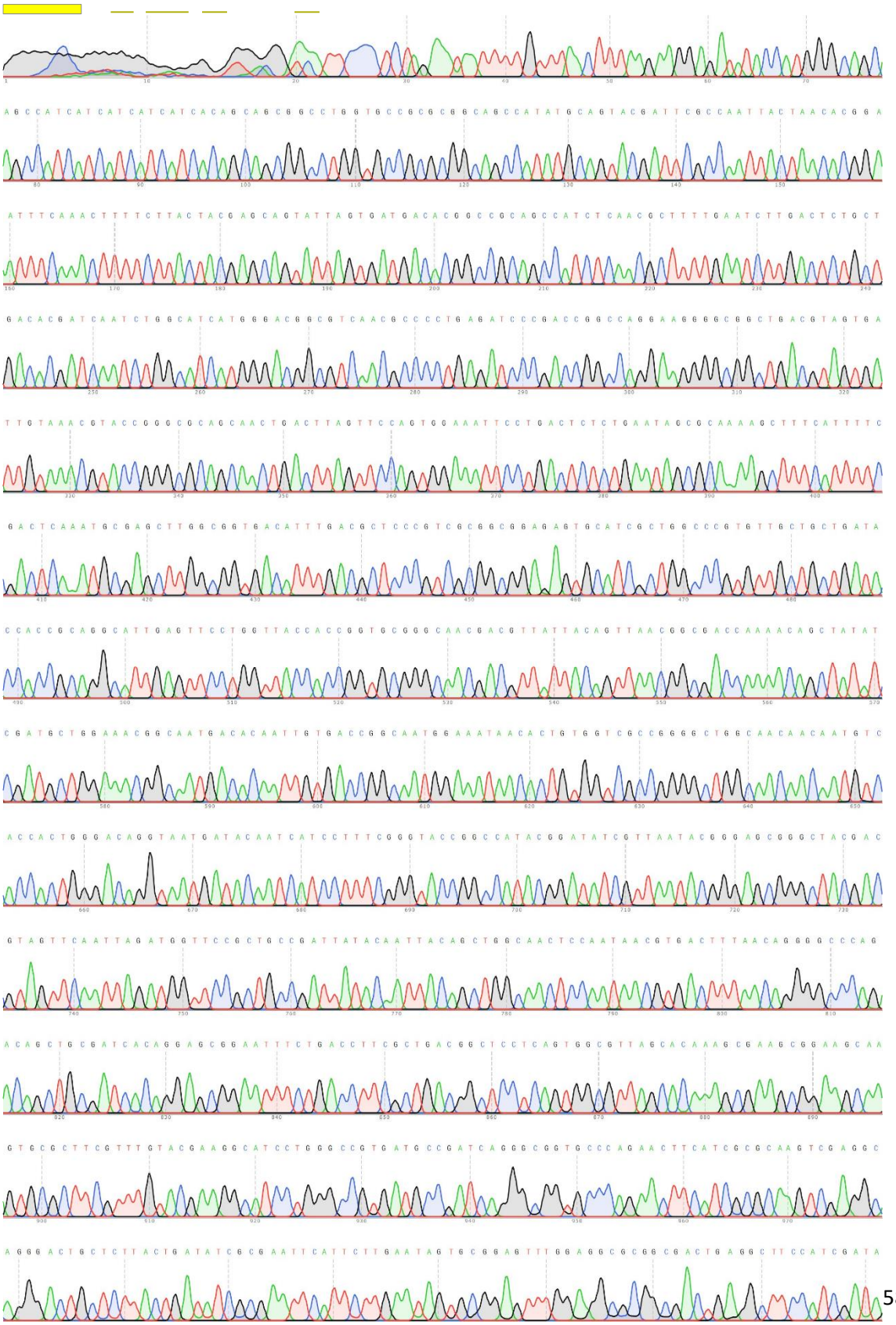

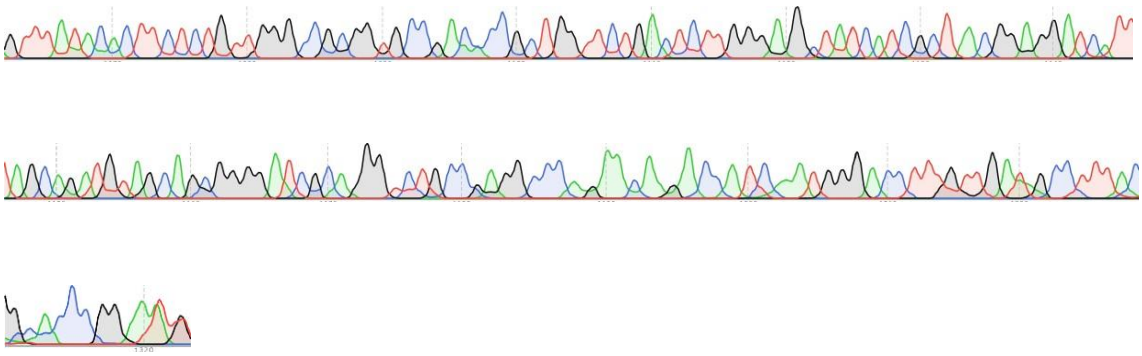

APPENDIX 2- Sequence Analysis Results for pET$_{28}$-AFP (Terminator)

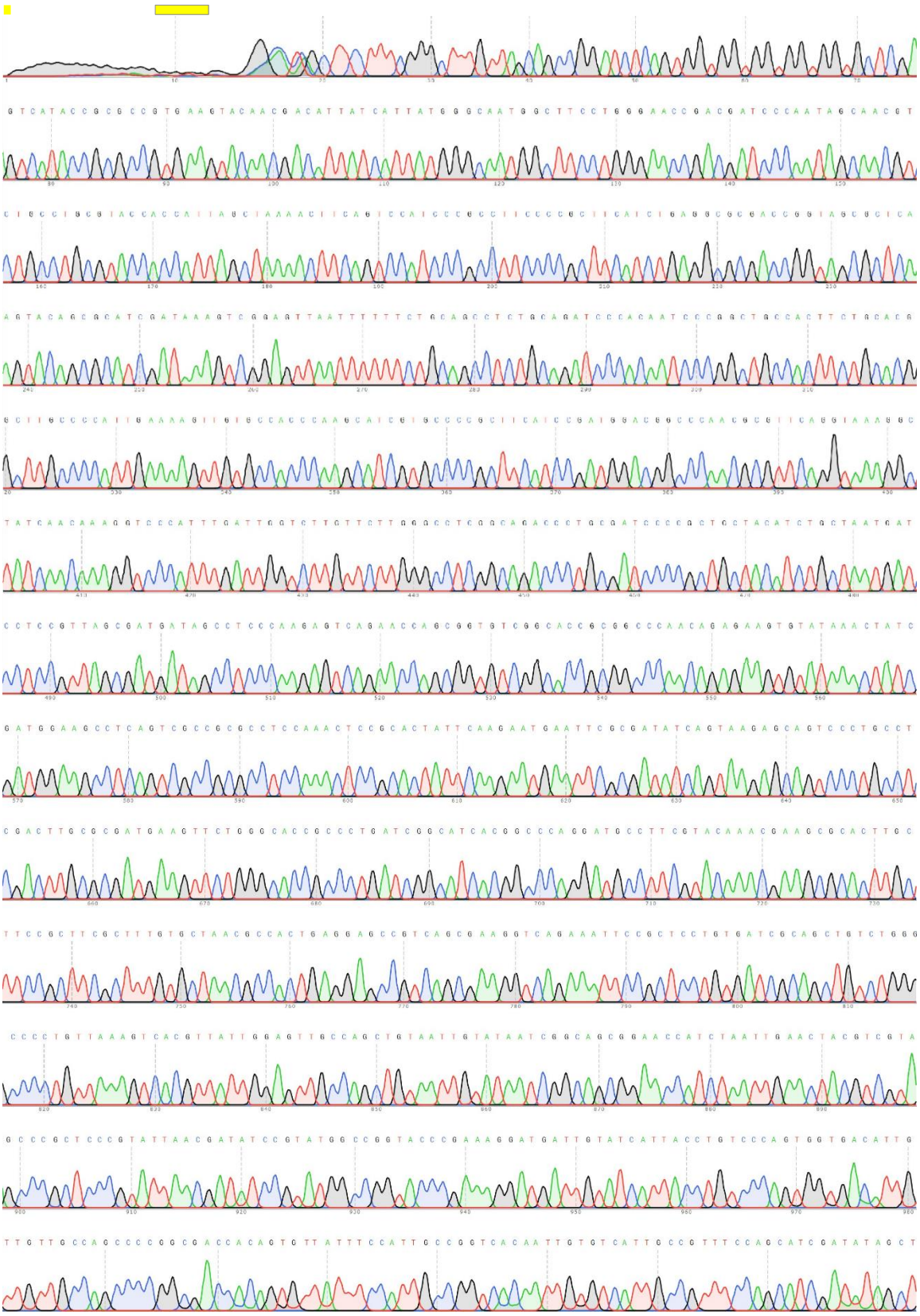

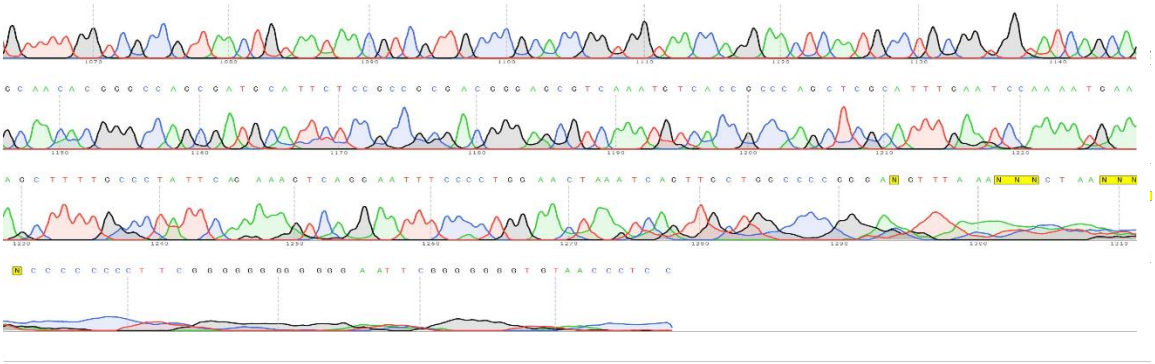

APPENDIX 3- Sequence Analysis Results for pET$_{21}$-AFP (Promoter)

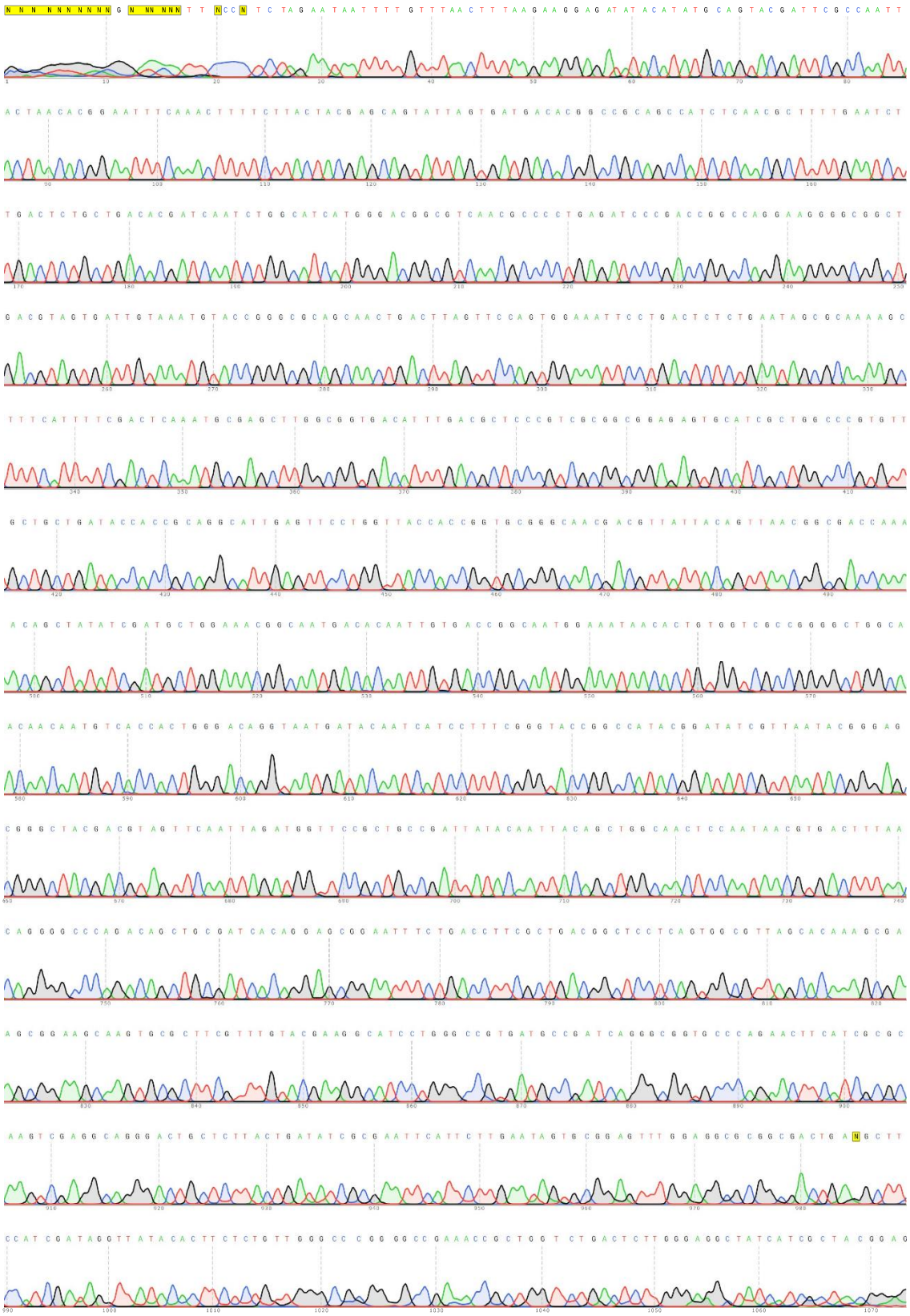

APPENDIX 4- Sequence Analysis Results for pET$_{21}$-AFP (Terminator)

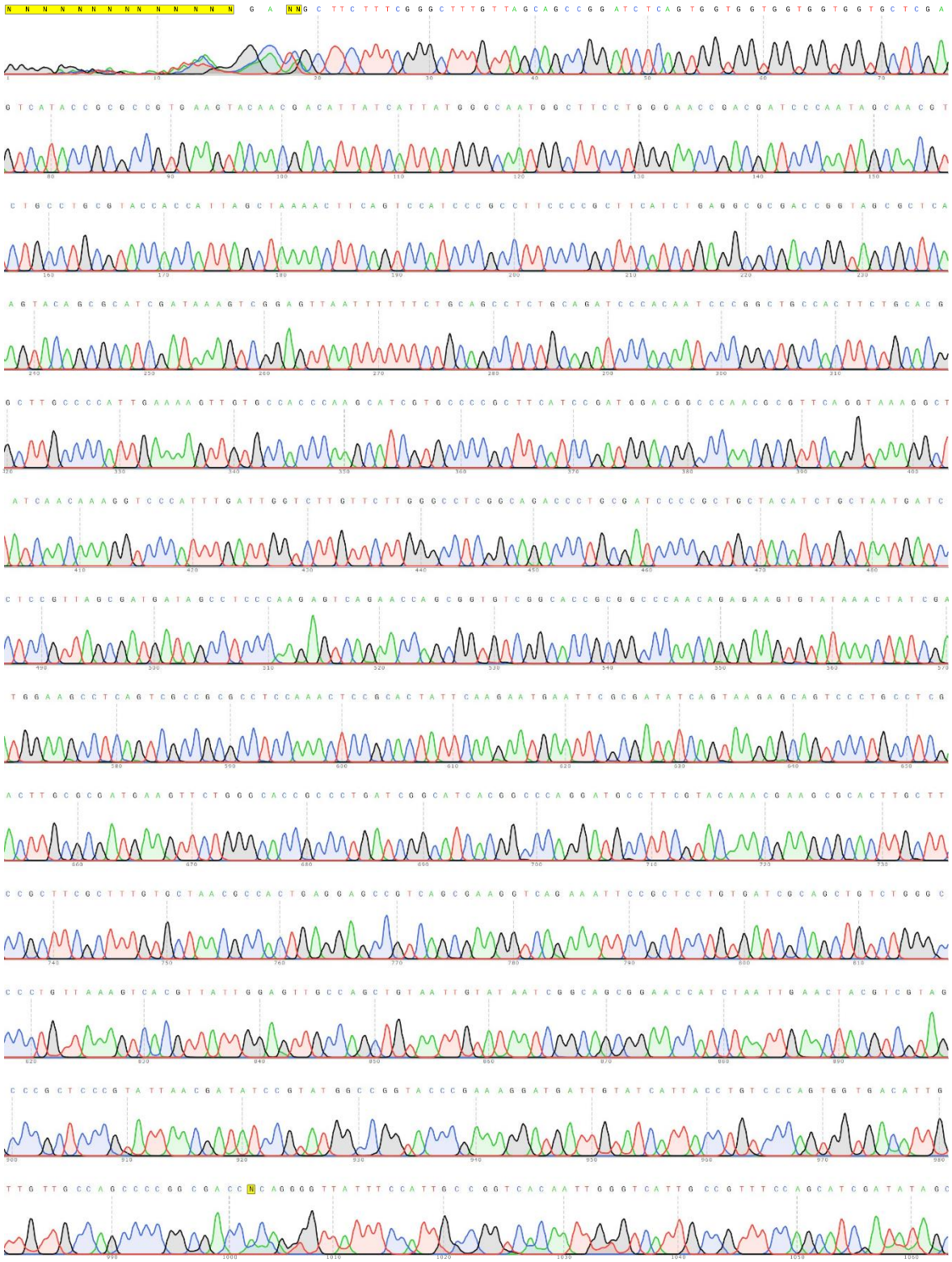

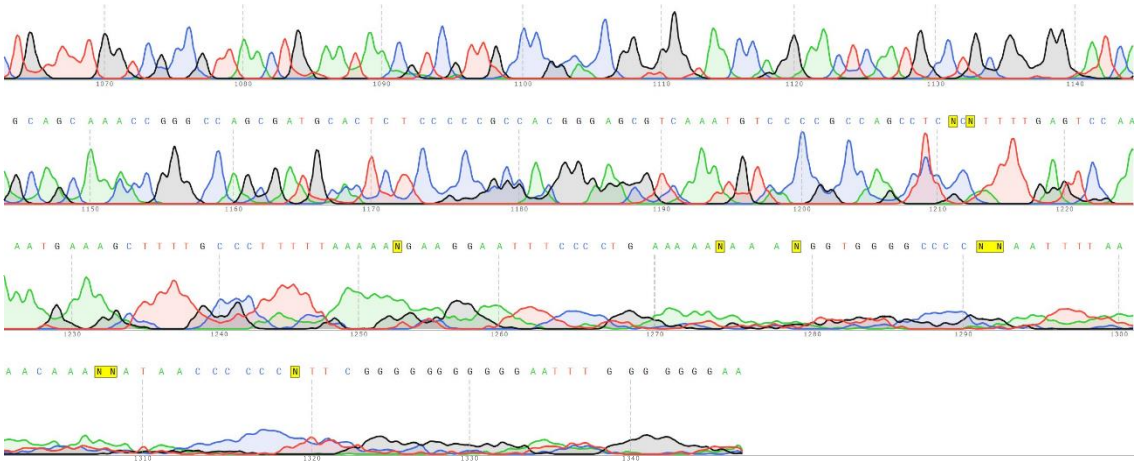

APPENDIX 5- Schematic of Experimental Setup of the Anti-icing Activity Tests